

2020

Investigation of Expedient, Cost Effective and Sustainable Soil Stabilization for Tactical Vehicles Using Surfactant-Induced Soil Stabilization (SISS)

Joshua Sasser
University of North Florida, jsasser7@gmail.com

Follow this and additional works at: <https://digitalcommons.unf.edu/etd>



Part of the [Civil Engineering Commons](#)

Suggested Citation

Sasser, Joshua, "Investigation of Expedient, Cost Effective and Sustainable Soil Stabilization for Tactical Vehicles Using Surfactant-Induced Soil Stabilization (SISS)" (2020). *UNF Graduate Theses and Dissertations*. 1000.

<https://digitalcommons.unf.edu/etd/1000>

This Master's Thesis is brought to you for free and open access by the Student Scholarship at UNF Digital Commons. It has been accepted for inclusion in UNF Graduate Theses and Dissertations by an authorized administrator of UNF Digital Commons. For more information, please contact [Digital Projects](#).

© 2020 All Rights Reserved

INVESTIGATION OF EXPEDIENT, COST EFFECTIVE AND SUSTAINABLE SOIL
STABILIZATION FOR TACTICAL VEHICLES USING SURFACTANT-INDUCED SOIL
STABILIZATION (SISS)

By

JOSHUA C. SASSER

A THESIS PRESENTED TO THE GRADUATE SCHOOL
OF THE UNIVERSITY OF NORTH FLORIDA IN PARTIAL FULFILLMENT
OF THE REQUIREMENTS FOR THE DEGREE OF
MASTER OF SCIENCE IN CIVIL ENGINEERING

UNIVERSITY OF NORTH FLORIDA

2020

This thesis titled "Investigation of Expedient, Cost Effective and Sustainable Soil Stabilization for Tactical Vehicles Using Surfactant-Induced Soil Stabilization (SISS)" written by Joshua C. Sasser has been approved by:

Raphael Crowley, PhD PE

Date

Donald Resio, PhD

Date

Ryan Shamet, PhD

Date

© 2020 JOSHUA C. SASSER

To my wife, Kati

ACKNOWLEDGMENTS

I would like to thank my incredibly supportive wife, Kati, and our two wonderful children for their support and love throughout this season of our lives. God has blessed me enormously and I am eternally grateful and undeserving.

I would like to thank my advisor, Dr. Raf Crowley for everything he does daily for the students and the Coastal Engineering program in general. His patience, kindness, and expertise have a tremendous impact on the program and certainly my experience here at UNF. His knowledge and guidance made this thesis possible. His commonsense approach, especially when tackling or explaining complex ideas, made me a better graduate student and undoubtedly a better engineer moving forward. Sincerely, thank you.

I would also like to thank Dr. Resio and the entire Taylor Engineering Research Institute (TERI) staff. This is a well led organization with an exceptional culture of inclusion and continuous improvement.

TABLE OF CONTENTS

	<u>page</u>
ACKNOWLEDGMENTS.....	5
LIST OF TABLES.....	8
LIST OF FIGURES	10
ABSTRACT.....	13
INTRODUCTION AND BACKGROUND.....	15
1.1 Why is Soil Stabilization Important?.....	15
1.2 Traditional Methods for Mitigating Soil Failure	17
1.2.1 Mechanical Stabilization	17
1.2.2 Admixtures	18
1.2.3 Geomicrobial Soil Improvement.....	20
1.2.4 Wick Drains	21
1.2.5 Increasing Bearing Area	21
1.2.6 Surfactant-Induced Soil Stabilization (SISS).....	22
1.3 Goals and Objectives.....	24
1.4 Thesis Organization.....	25
METHODOLOGY.....	26
2.1 Background	26
2.2 Sediment Characteristics	26
2.3 Chemical Characteristics	27
2.4 Cylinder Testing.....	29
2.4.1 Cylinder Preparation.....	29
2.4.2 Cylinder Mixing Procedures	31
2.4.3 UCS Testing Procedure.....	33
2.5 Sandbox Testing.....	35
2.5.1 Sandbox Preparation.....	35
2.5.2 Sandbox Treatment Procedure.....	37
2.5.3 Pocket Penetrometer Testing	38
2.5.4 Traction testing.....	39
2.5.5 Crust Depth Testing	42
2.6 Dissolution Testing	43
2.6.1 Specimen Preparation	43
2.6.2 Testing Procedure	44
RESULTS	45
3.1 Unconfined Compression Test Results	45
3.2 Sand Box Results	47

3.2.1 Pocket Penetrometer Testing	47
3.2.2 Traction	51
3.2.3 Crust Depth	55
3.3 Dissolution	57
DISCUSSION	59
4.1 Data Analysis – Strength Testing	59
4.2 Data Analysis – Traction Testing	65
4.3 Data Analysis – Crust Depth	69
4.4 Data Analysis – Dissolution Testing	71
4.5 Implications for Upscaling to Field Application	72
CONCLUSIONS	75
5.1 Summary	75
5.3 Preliminary Conclusions	75
5.3 Recommendations for Future Testing	76
LIST OF REFERENCES	77
BIOGRAPHICAL SKETCH	80

LIST OF TABLES

<u>Table</u>	<u>page</u>
Table 2-1. Specifications for mixing the constituents for Round One of UCS testing using SDS in powder form.....	30
Table 2-2. Specifications for mixing the constituents for Round Two of UCS testing using SDS as a 20% aqueous solution.....	30
Table 2-3. Specifications for mixing the constituents for Round Three of UCS testing using SDS in powder form.....	31
Table 2-4. Specifications for mixing constituents for Round One of box testing using SDS as a 20% solution and CaCl ₂ as a 2.5M solution.	36
Table 2-5. Specifications for mixing constituents for Round Two of box testing using SDS as a 20% solution and CaCl ₂ as a 0.5M solution.	36
Table 2-6. Specifications for mixing constituents for Control box testing using SDS as a 20% solution and CaCl ₂ as a 2.5M solution.	36
Table 2-7. Properties of the single wheel traction testing vehicle	42
Table 2-8. Properties of a High Mobility Multipurpose Wheeled Vehicle (HMMWV).	42
Table 2-9. Dissolution Testing Matrix	43
Table 3-1. Consolidated Results of UCS Testing	45
Table 3-2. Pocket Penetrometer Results (20% SDS solution // 2.5M CaCl ₂ solution) ..	48
Table 3-3. Pocket Penetrometer Results (20% SDS solution // 0.5M CaCl ₂ solution) ..	49
Table 3-4. Pocket Penetrometer Results (Control Tests)	50
Table 3-5. Max Sinkage (20% SDS solution // 2.5M CaCl ₂ solution).....	51
Table 3-6. Sinkage Rates (20% SDS solution // 2.5M CaCl ₂ solution).....	51
Table 3-7. Max Sinkage (20% SDS solution // 0.5M CaCl ₂ solution).....	52
Table 3-8. Sinkage Rates (20% SDS solution // 0.5M CaCl ₂ solution).....	53
Table 3-9. Max Sinkage (Control Tests).....	54
Table 3-10. Sinkage Rates (Control Tests)	54
Table 3-11. Crust Depth (20% SDS solution // 2.5M CaCl ₂ solution)	56

Table 3-12. Crust Depth (20% SDS solution // 0.5M CaCl ₂ solution)	56
Table 3-13. Crust Depth (Control Tests)	57
Table 3-14. Dissolution Results.....	58
Table 4-1. Maximum Average Compressive Strength Results from each testing series	60
Table 4-2. Rate of sinkage (i.e., sinkage slope) from sandbox testing Round 1 (20% SDS // 2.5M CaCl ₂)	67
Table 4-3. Rate of sinkage (i.e., sinkage slope) from sandbox testing Round 2 (20% SDS // 0.5M CaCl ₂)	67

LIST OF FIGURES

<u>Figure</u>	<u>page</u>
Figure 1-1: Example of collapsed building in India (Geoengineer.org, 2020).....	15
Figure 1-2: Collapsed house in Vilano Beach as a result of erosion from Hurricane Irma.....	16
Figure 1-3: (Left) Failed dune crest despite the use of sod. (Right) Bulkhead wingwall failure.....	16
Figure 1-4. High Mobility Multipurpose Wheeled Vehicle (HMMWV) stuck in the sand during an amphibious exercise in Portugal in 2015. (sputniknews.com) ...	17
Figure 1-5. Various types of shallow compaction equipment (Ebid, 2018).....	18
Figure 1-6. Typical soil-cement additive mix equipment (CSFE, 2010).....	19
Figure 1-7. Example of wick drain with preload in place (Wikar, 2018).....	21
Figure 1-8: (Left) US Marines installing AM2 matting (Hollis, 2014). (Right) Load test of AM2 matting placed over sand (Rushing et al, 2014).	22
Figure 1-9. Depiction showing the structure of a micelle and reverse micelle (Schmitz, 2018).	23
Figure 1-10. Depiction of a calcium dodecyl sulfate complex with soil particles absorbed into the center of the micelles (Crowley et al, 2019).....	23
Figure 2-1. Grain-Size Distribution used in this study (adapted from Chek 2019).....	27
Figure 2-2. Cylinders in drying oven.....	32
Figure 2-3. ELE International Hand Operated Unconfined Compression Tester, Model 25-3602.	33
Figure 2-4. UCS testing in progress	34
Figure 2-5. Photograph showing sandbox SDS application (Top left), CaCl ₂ (Top right), and (Bottom) the sandboxes immediately following treatment.	37
Figure 2-6. Photo of the pocket penetrometer used for this study.	38
Figure 2-7. Photo of compressive strength testing being conducted using pocket penetrometer.	39
Figure 2-8. Wheel soil interaction model (Reina et al 2006).	40

Figure 2-9. (Left) Photo of the single wheel traction tester prepared for testing. (Right) Photo showing the rut caused by traction testing.	41
Figure 2-10. Photo showing the top crust formed as a result of SISS treatment in a sandbox.	43
Figure 2-11. (Left) Photo of the specimens cut out of the sand box treated with 10.75% of the PV filled with SDS for test D-6. (Right) Photo showing the side-by-side dissolution testing of test D-6.	44
Figure 3-1. Plot summary of UCS Results (note – results from UCTP2-1 removed as an outlier)	46
Figure 3-2. Best fit curve of UCS Results. Note: Regression only applies within the bounds of the dataset.	47
Figure 3-3. Pocket Penetrometer Results (20% SDS solution // 2.5M CaCl ₂ solution). Note: Symbols denote averages, wings denote standard deviations.	48
Figure 3-4. Pocket Penetrometer Results (20% SDS solution // 0.5M CaCl ₂ solution). Note: Symbols denote averages, wings denote standard deviations. X-axis not to scale.	49
Figure 3-5. Pocket Penetrometer Results (Control Tests). Note: Symbols denote averages, wings denote standard deviations. X-axis not to scale.	50
Figure 3-6. Sinkage Rates (20% SDS solution // 2.5M CaCl ₂ solution)	52
Figure 3-7. Sinkage Rates (20% SDS solution // 0.5M CaCl ₂ solution)	53
Figure 3-8. Sinkage Rates (Control Tests)	55
Figure 3-9. Crust Depth Results from Round Two of Testing (20% SDS solution // 0.5M CaCl ₂ solution). Note: Regression only applies within the bounds of the dataset.	56
Figure 3-10. Crust Depth Results from Control Testing. Note: Regression only applies within the bounds of the dataset.	57
Figure 4-1. Plot of compressive strength vs SDS quantity for sandbox testing Round 2 (20% SDS // 0.5M CaCl ₂). Note: Compressive strength values are 21 day averages from penetrometer testing. Regression only applies within the bounds of the dataset.	62
Figure 4-2. Plots of penetrometer results from Round 1 of sandbox testing (20% SDS solution // 2.5M CaCl ₂ solution). Standard deviation as a function of SDS quantity.	63

Figure 4-3. Plots of penetrometer results from Round 2 of sandbox testing (20% SDS solution // 0.5M CaCl ₂ solution). Standard deviation as a function of SDS quantity.	64
Figure 4-4. Plots of penetrometer results from Control sandbox testing. Standard deviation as a function of SDS quantity.	65
Figure 4-5. Plot of Time to Max Rut Depth results. Note: Regression only applies within the bounds of each dataset.	67
Figure 4-6. Rate of sinkage plotted as a function of SDS quantity. Note: Regression only applies within the bounds of each dataset.	68
Figure 4-7. Rate of sinkage plotted as a function of Compressive Strength. Results from Round 2 of sandbox testing (20% SDS solution // 0.5M CaCl ₂ solution). Note: Regression only applies within the bounds of the dataset.	68
Figure 4-8. Plot of compressive strength vs crust depth for round 2 of sandbox testing (20% SDS solution // 0.5M CaCl ₂ solution). Note: Regression only applies within the bounds of the dataset.	69
Figure 4-9. Plot of compressive strength vs crust depth for Control sandbox testing. Note: Regression only applies within the bounds of the dataset.	70
Figure 4-10. Plot of dissolution time vs SDS quantity.	72

Abstract of Dissertation Presented to the Graduate School
of the University of North Florida in Partial Fulfillment of the
Requirements for the Degree of Master of Science in Civil Engineering

INVESTIGATION OF EXPEDIENT, COST EFFECTIVE AND SUSTAINABLE SOIL
STABILIZATION FOR TACTICAL VEHICLES USING SURFACTANT-INDUCED SOIL
STABILIZATION (SISS)

By

Joshua C. Sasser

December 2020

Chair: Raphael Crowley, PhD PE
Major: Civil Engineering

Surfactant-induced soil stabilization (SISS) is a new method for soil stabilization whereby anionic surfactants and alkaline earth metals are introduced to a soil matrix. This research served as a preliminary study into SISS' suitability as a temporary soil stabilization method that could be used to improve wheeled vehicle traction during amphibious type naval operations conducted on a beach head.

Beach sand specimens were treated with sodium dodecyl sulfate (SDS; aka sodium lauryl sulfate) and calcium chloride using two methods: hand mixing in testing cylinders and surface percolation in bench scale sandboxes. Treated cylinders were tested for unconfined compressive strength (UCS) and treated sandboxes were tested for compressive strength, traction, treatment depth, and dissolution. Cylinder testing results appear to show a parabolic relationship between SDS content and UCS with an estimated local maximum of 48.4 psi corresponding to 81.4% of the pore volume (PV) filled with SDS. Sandbox testing results appear to show that the surface percolation treatment method can offer similar compressive strength improvements while using considerably less SDS. These strength improvements appear to also result in improved

resistance to wheeled vehicle sinkage. Dissolution results show that beach sand treated with both SDS and CaCl₂ tended to be resistive to dissolution in both seawater and distilled water.

Overall, the results of this preliminary study show that SISS may provide compressive strength improvements and traction improvements in beach sand. These results are encouraging however they are strictly bench-scale and also showed significant variability, therefore additional research is required.

CHAPTER 1 INTRODUCTION AND BACKGROUND

1.1 Why is Soil Stabilization Important?

Soil is a highly heterogenous nonisotropic material. Like any material, a given soil matrix has a certain stiffness and strength. If strength and/or stiffness are incapable of supporting the loads upon the soil, the soil will fail and may cause damage. Anecdotal accounts of these sorts of failures are abundant in the literature (Cummings & Kenton, 2004). In June of 2020 a three-story building collapsed in India (Fig. 1-1).



Figure 1-1: Example of collapsed building in India (Geoengineer.org, 2020)

This is an example of structural scour where a nearby channel undercut the structure's foundation. Scour damage ultimately led to the building's collapse.

Locally, several instances of severe damage due to soil failure were documented as a result of Hurricanes Matthew and Irma (Hudyma et al. 2017; Landon et al. 2020; Crowley et al. 2018). Crowley et al. found in their 2018 study that relatively few strategies were used for erosion defense along the northeast Florida coastline prior to

the storms. The strategies that were used were largely ineffective; significant dune erosion occurred; several structural foundations were undermined/scoured; and damage from these events cost millions of dollars. Fig 1-2 through Fig 1-3 are photos taken in northeast Florida during damage assessment of Hurricane Irma (Hudyma et al. 2017).



Figure 1-2: Collapsed house in Vilano Beach as a result of erosion from Hurricane Irma.



Figure 1-3: (Left) Failed dune crest despite the use of sod. (Right) Bulkhead wingwall failure.

Direct loading upon a soil surface may also cause the soil to fail. One instance of direct loading that is of particular interest is wheeled vehicle loading upon sandy soil surfaces. The United States military utilizes a wide array of vehicles of varying size,

weight, and purpose. Rubber tire vehicles are heavily utilized due to their versatility and performance at high speed. Generally, these vehicles perform very well over hard surfaces. However, these vehicles tend to perform very poorly when used on soft soil surfaces such as beach heads. As shown below in Fig. 1-4, heavier, rubber-tire vehicles are subject to “sink in the sand” when deployed to a beach. This presents issues for expedient offloading during beach exercises and amphibious landing operations.



Figure 1-4. High Mobility Multipurpose Wheeled Vehicle (HMMWV) stuck in the sand during an amphibious exercise in Portugal in 2015. (sputniknews.com)

1.2 Traditional Methods for Mitigating Soil Failure

Mitigating soil failure due to scour/erosion (Fig. 1-1 through Fig. 1-3) or due to direct loading (Fig. 1-4) is a relatively robust field. Several methods are available that are discussed below:

1.2.1 Mechanical Stabilization

Mechanical stabilization is the process of improving the properties of the soil by changing its gradation by way of compaction and densification using mechanical energy

from various types of equipment (Habiba, 2017). Mechanical soil stabilization often involves the installation of reinforcement, such as geogrid, at multiple levels within the soil column and performing compaction at each level. Compaction alone can be extremely effective at improving the bearing capacity of soil. For this method to be most effective, engineers specify the type of soil to be used and an optimum moisture content. While effective, compaction tends to be extremely labor intensive and expensive. The compaction equipment pictured in Fig 1-5 are commonly used as part of the mechanical stabilization process.



Figure 1-5. Various types of shallow compaction equipment (Ebid, 2018).

1.2.2 Admixtures

Stabilization through admixtures is the process of adding substances to the soil to improve various properties such as volume stability, strength, compressibility,

permeability and durability. There are many different types of admixtures that can be introduced to the soil including lime, cement, chemicals, fly ash, bituminous materials, thermal energy, electrical energy, geotextiles and recycled/waste products (Habiba 2017). Fig. 1-6 below illustrates some typical equipment used for supplementing soils with admixtures.



Figure 1-6. Typical soil-cement additive mix equipment (CSFE, 2010).

Commercially, many proprietary products are available that may be applied to the soil, either topically or through mechanical mixing. Examples include OPSDIRT®, Global Road Technology: Enviro Binder®, and Envirotac II® (Rhino Snot). All these methods provide various levels of effectiveness depending on the soil properties, desired outcome and method of application. However, the issue with most of these admixture techniques is that they tend to be expensive and/or environmentally harmful.

In addition, when used in an environmentally sensitive environments, the long-lasting effects associated with most admixture treatments are often seen as a drawback.

1.2.3 Geomicrobial Soil Improvement

Recently, geomicrobial soil improvement, particularly microbially-induced calcite precipitation (MICP) and enzyme-induced calcite precipitation (EICP), have emerged as new soil stabilization methods. Both MICP and EICP are similar in the sense that each utilizes urease to lyse urea. The resultant urea lyses eventually results in production of calcium carbonate and the calcium carbonate binds soil particles together. This technique is promising because it is sustainable. The downside to MICP treatment is that geomicrobes are required. If soil is augmented with additional microbes, the augmented microbes may be overwhelmed by the soil's native microbiota; or the microbes may simply die for other reasons. A study performed by Martin et al. (2012) has also shown that typical microbes used for MICP may not produce urease under anoxic conditions. As such, relative effectiveness may be limited to situations where the geomicrobes are exposed to air near the soil surface. EICP is a sort of "work-around" to the microbe problem in the sense that urease may be synthesized directly (usually from soybeans). However, urease extraction may be expensive and time consuming. Both MICP and EICP are exciting technologies that have been shown to effectively strengthen relatively clean sands. However, when used in other soils like clays or soils with high organic matter, their effectiveness is limited (Davies et al. 2019). Furthermore, each of these technologies may be expensive and difficult to implement on a large-scale.

1.2.4 Wick Drains

Wick drains are typically prefabricated earth drains that are installed in the soil to reduce the consolidation time by shortening the drainage path of compressible materials which typically have poor drainage properties such as clayey soils (Mullins and Gunaratne, 2015). While these may function effectively in cohesive soils, they are irrelevant in sands as sands drain naturally. An illustration of wick draining is shown below in Fig. 1-7.

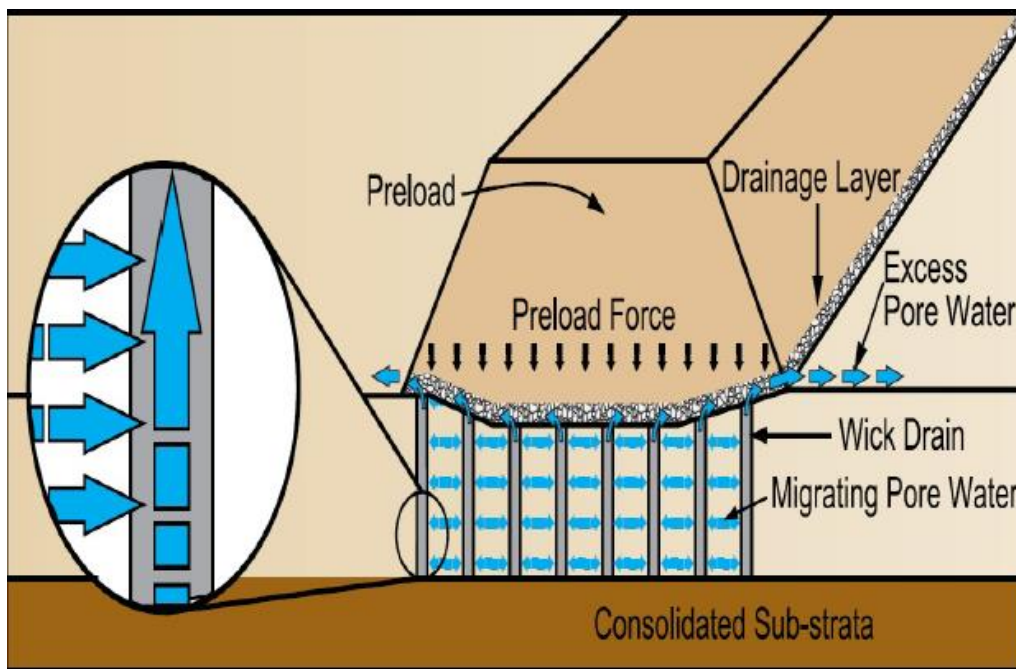


Figure 1-7. Example of wick drain with preload in place (Wikar, 2018).

1.2.5 Increasing Bearing Area

Increasing the bearing area is the process of leaving the existing soil conditions unchanged and reducing stress upon the soil by increasing the bearing area over which the loads are applied. Examples of this include large, widespread foundations for buildings and matting for vehicle traffic. A frequently used product in military applications is aluminum matting, commonly referred to as AM2 matting (Fig. 1-8). AM2

matting can be used for everything from tent floors to expeditionary runways. This is an effective solution; however, it is extremely labor intensive and requires a large amount of matting which is expensive, heavy, takes up a large amount of space when not in use, and must be recovered after use.



Figure 1-8: (Left) US Marines installing AM2 matting (Hollis, 2014). (Right) Load test of AM2 matting placed over sand (Rushing et al, 2014).

1.2.6 Surfactant-Induced Soil Stabilization (SISS)

In recent years, a new method for soil stabilization has been developed dubbed Surfactant-Induced Soil Stabilization (SISS; Crowley et al. 2020). SISS is a relatively simple technology whereby anionic surfactants, particularly sodium dodecyl sulfate (SDS; aka sodium lauryl sulfate) are introduced to a soil matrix. Then, alkaline earth metals (usually calcium although magnesium and strontium are also effective) are introduced. The surfactant tends to form micelles when above the critical micelle count (CMC; Fig. 1-9) and soil particles either tend to become surrounded by the micelles (Fig. 1-10); or the micelles embed themselves in the soil's void spaces. Regardless of whether the micelles encapsulate the soil particles or reside in the soil void spaces,

ultimately, they are bound together by the alkaline earth metal ions. The result is a strengthened soil matrix.

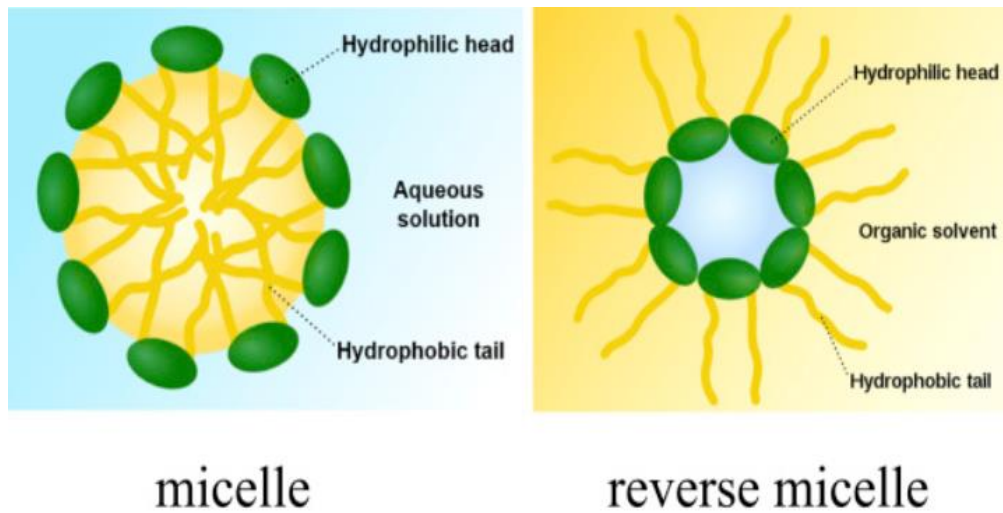


Figure 1-9. Depiction showing the structure of a micelle and reverse micelle (Schmitz, 2018).

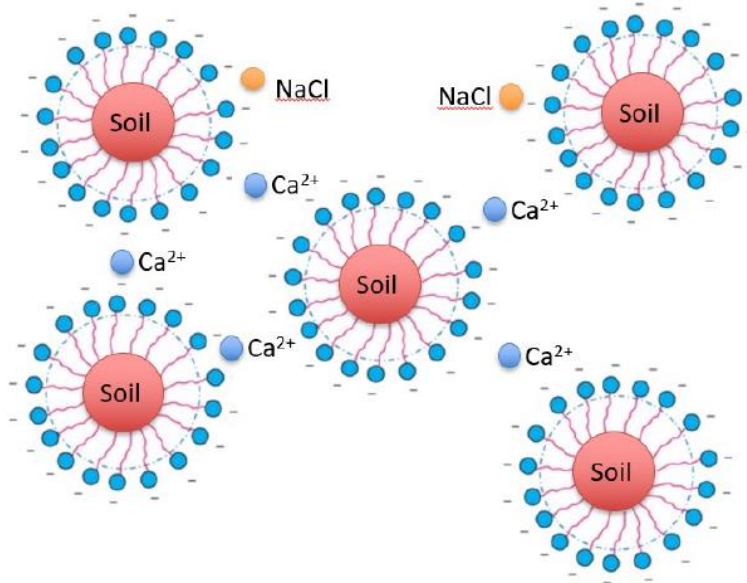


Figure 1-10. Depiction of a calcium dodecyl sulfate complex with soil particles absorbed into the center of the micelles (Crowley et al, 2019).

Preliminary data suggest that under dry and freshwater saturated conditions, the resultant surfactant-soil matrix has proven to be relatively insoluble, and that under saltwater conditions, sodium from saltwater's sodium chloride tends to replace the calcium ions that bind the surfactant micelles together (Davies 2018). Thus, when introduced to saltwater, the soil tends to become destabilized and return to its native state. Usually, this sort of behavior would be considered undesirable in the sense that usually engineers wish to improve soil permanently. However, in the context of military beachhead operations, the goal may be to achieve temporary stabilization while operations are conducted; and then for the beach to "return to normal" shortly thereafter. SISS may be a technology that could be used to achieve these objectives.

1.3 Goals and Objectives

The goal of this research was to provide a preliminary assessment of SISS' suitability for use as a temporary soil stabilization method that could be used during amphibious type operations conducted on a beach head. In particular, strength improvement and traction improvement were examined in the context of optimizing SISS constituent quantities. Davies (2018) provided some preliminary strength data; the first goal of this thesis was to supplement these data and generate more information about optimal quantities of SDS and calcium in beach sand. The second phase of this research involved upscaling SISS treatment to bench-scales using treatment techniques that could be feasibly applied in the field. During this second phase of research, tire rut formation was examined and qualitatively compared for beach sands that were treated with different quantities of SISS constituents. This research concluded with a further examination of SISS-treated soil's dissolvability in both freshwater and saltwater.

1.4 Thesis Organization

This thesis is organized into chapters as follows:

- Chapter 2 presents the methodology, the materials and testing methods used throughout this research.
- Chapter 3 presents the results from the various tests completed.
- Chapter 4 presents analysis of the results shown in Chapter 3.
- Chapter 5 presents a summary, conclusions and future recommendations.

CHAPTER 2 METHODOLOGY

2.1 Background

As discussed in Chapter 1, the goal of this study was to conduct a preliminary assessment of the SISS method. More specifically, the goal was to quantify strength and traction improvements and determine optimum SISS constituent quantities. As such, three testing series were conducted:

1. Initial Cylinder Testing. Several 2 in by 4 in cylinders were filled with beach sand and treated with SDS and calcium chloride of varying quantities. Then, the treated cylinders were extracted and their unconfined compressive strengths (UCS) were tested. The purpose of these tests was to optimize SDS and calcium chloride as a function of void ratio.
2. Bench-scale Sandbox Testing. Several 5.5 in by 5.5 in by 5.5 in bench-scale sandboxes were filled with beach sand and treated with SDS and calcium chloride using a surface percolation technique. The purpose of this test-series was to gauge effectiveness of surface percolation treatment because this sort of treatment technique can be upscaled for field use. These boxes were tested for surface strength using a surface penetrometer and traction using a homemade traction test. In addition, effective treatment depth was estimated by measuring the depth of the hardened crust that formed below the soil surface.
3. Dissolution Cylinder Testing. Several 2 in by 4 in cylinders were filled with beach sand and treated using the SISS technique. Dissolution was studied in both submerging several of these cylinders in both freshwater and saltwater.

2.2 Sediment Characteristics

The sediment used for this research was beach sand from Atlantic Beach, FL and was taken from the same location as Chek et al. (2020). The sediment distribution associated with this sand is shown below in Fig. 2-1:

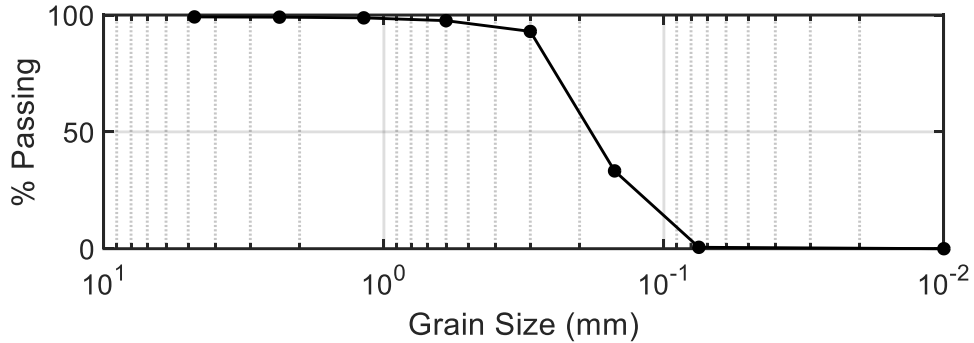


Figure 2-1. Grain-Size Distribution used in this study (adapted from Chek 2019)

Chek (2019) measured void ratio in accordance with ASTM C136/C136M-14 (ASTM 2014); the soil's void ratio, e , is 0.36. This void ratio was used in this study to determine the volume of voids in each testing series. From the void ratio, the porosity, n was calculated using Equation 2.1.

$$n = \frac{e}{1+e} = \frac{0.36}{1+0.36} = 0.26 \quad (2-1)$$

The density, ρ_s , was determined by measuring the mass of the sand in a 2 in by 4 in cylinder (306.1 g), and dividing by the volume of the cylinder (205.93 cc) to yield a density of 1.49 g/cc. The void volume for each testing series was determine using Equation 2.2.

$$V_v = nV_t \quad (2-2)$$

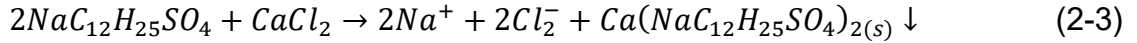
where V_v represents the void volume and V_t represents the total volume.

2.3 Chemical Characteristics

The surfactant used for this study was sodium dodecyl sulfate (SDS), whose chemical formula is $NaC_{12}H_{25}SO_4$. Tests were conducted using SDS in both the powder and aqueous solution form. The aqueous solution was diluted with distilled water to 20% by weight. This SDS concentration was used because it is the strongest concentration

that is readily premixed and commonly commercially available. The alkaline earth metal used was calcium in the form of calcium chloride (CaCl₂). The CaCl₂ was diluted using distilled water to either a 2.5 molar solution or a 0.5 molar solution depending on the testing series.

The governing reaction associated with SISS treatment is believed to be:



As such, SDS and CaCl₂ were initially stoichiometrically balanced using a 2:1 chemical ratio. As shown below in Eq. 2-4, this balance led to 5.2 g of SDS per gram of CaCl₂:

$$MR = \frac{MW_{SDS} \left(\frac{288.372\text{-g}}{\text{mol}} \right) \times 2\text{mols}}{MW_{CaCl_2} \left(\frac{110.98\text{-g}}{\text{mol}} \right) \times 1\text{mol}} = 5.2 \quad (2-4)$$

where *MR* denotes the molar ratio and *MW_{SDS}* and *MW_{CaCl₂}* represent the molar weights of SDS and CaCl₂ respectively. For each test, SDS quantity varied and was expressed as a function of percentage of filled pore volume, *PV*. The computations associated with determining appropriate volumes of each constituent are presented below from Eq. 2-5 through Eq. 2-8:

$$m_{SDS} = (\%PV)(V_v)(\rho) \quad (2-5)$$

$$m_{CaCl_2} = \frac{m_{SDS}}{MR} \quad (2-6)$$

$$V_{SDS} = \frac{m_{SDS}}{\%SDS} \quad (2-7)$$

$$V_{CaCl_2(s)} = \frac{m_{CaCl_2}}{M_{CaCl_2} MW_{CaCl_2}} \quad (2-8)$$

$$V_{CaCl_2(a)} = \frac{m_{CaCl_2}}{M_{CaCl_2} MW_{CaCl_2}} \quad (2-9)$$

where m , MW , and V denote masses, molecular weight, and volumes for each constituent respectively. Subscripts s and a denote solid (i.e., precipitate) and aqueous respectively.

2.4 Cylinder Testing

Three rounds of cylinder testing were conducted. The first round of testing was completed using SDS powder. The second series utilized aqueous SDS solution with 20% molarity. The third sequence utilized powder once again. The following describes the testing procedures associated with each of these tests.

2.4.1 Cylinder Preparation

Based upon prior experience, the goal was to fill each 2 in by 4 in test cylinder approximately halfway with soil to allow for sufficient space for adding the SISS constituents and mixing. Each cylinder's total volume was approximately 206 cc. Based upon the sand's density (1.49 g/cc), 150 g of sand yields approximately 100.91 cc, which is approximately half each cylinder's volume. Thus 150 g of sand was used for each cylinder test. Then, SDS quantities were specified as a function of PV , and the appropriate masses and volumes of SDS and CaCl_2 were computed using Eq. 2-5 through Eq. 2-9. The result of this computation is presented below in Table 2-1 through Table 2-3:

Table 2-1. Specifications for mixing the constituents for Round One of UCS testing using SDS in powder form

Test #	% PV filled by SDS	Total % of PV Filled	Mass of SDS Powder (g)	Mass of CaCl ₂ Powder (g)	V CaCl ₂ Solution (cc)
UCTP1-1	14%	24%	3.82	0.73	2.65
UCTP1-2	28%	48%	7.64	1.47	5.30
UCTP1-3	42%	72%	11.45	2.20	7.94
UCTP1-4	57%	96%	15.27	2.94	10.59
UCTP1-5	71%	120%	19.09	3.67	13.24
UCTP1-6	85%	144%	22.91	4.41	15.89
UCTP1-7	99%	168%	26.73	5.14	18.54
UCTP1-8	113%	193%	30.55	5.88	21.19
UCTP1-9	127%	217%	34.36	6.61	23.83
UCTP1-10	142%	241%	38.18	7.35	26.48

Table 2-2. Specifications for mixing the constituents for Round Two of UCS testing using SDS as a 20% aqueous solution

Test #	% of PV filled by SDS	Total % of PV Filled	Mass of SDS Powder (g)	V 20% SDS Solution (cc)	Mass of CaCl ₂ Powder (g)	V CaCl ₂ - 2.5M Solution (cc)
UCSS-1	4%	24%	1.13	5.65	0.22	0.78
UCSS-2	8%	48%	2.26	11.29	0.43	1.57
UCSS-3	13%	72%	3.39	16.94	0.65	2.35
UCSS-4	17%	96%	4.52	22.58	0.87	3.13
UCSS-5	21%	120%	5.65	28.23	1.09	3.92
UCSS-6	25%	144%	6.77	33.87	1.30	4.70
UCSS-7	29%	168%	7.90	39.52	1.52	5.48
UCSS-8	33%	193%	9.03	45.16	1.74	6.26
UCSS-9	38%	217%	10.16	50.81	1.96	7.05
UCSS-10	42%	241%	11.29	56.45	2.17	7.83

Table 2-3. Specifications for mixing the constituents for Round Three of UCS testing using SDS in powder form

Test #	% of PV Filled by SDS	% of PV Filled	Mass of SDS Powder (g)	Mass of CaCl ₂ Powder (g)	V CaCl ₂ - 2.5M Solution (cc)
UCSP2-1	28%	47%	7.50	1.44	5.20
UCSP2-2	36%	61%	9.75	1.88	6.76
UCSP2-3	44%	76%	12.00	2.31	8.32
UCSP2-4	53%	90%	14.25	2.74	9.88
UCSP2-5	61%	104%	16.50	3.18	11.44
UCSP2-6	69%	118%	18.75	3.61	13.00
UCSP2-7	78%	132%	21.00	4.04	14.56
UCSP2-8	86%	147%	23.25	4.47	16.13
UCSP2-9	95%	161%	25.50	4.91	17.69
UCSP2-10	103%	175%	27.75	5.34	19.25
UCSP2-11	111%	189%	30.00	5.77	20.81

2.4.2 Cylinder Mixing Procedures

The procedures for mixing the testing cylinders was as follows for the test-series using SDS in powder form (test-series UCTP1 and UCSP2):

1. The appropriate mass of SDS powder was added to a mixing bowl and small clumps of material were broken up by hand.
2. 150g of beach sand were added to the mixing bowl and mixed thoroughly with the SDS.
3. The mixture was transferred to a 2 in by 4 in testing cylinder.
4. The appropriate volume of CaCl₂ solution was added to the cylinder and mixed thoroughly using a spatula.
5. Once all constituents have been fully mixed, the top of each cylinder was screeded.

Note that appropriate safety gear was utilized throughout. Specifically, a respirator was worn at all times to avoid inhaling SDS and irritating the respiratory tract. The following is the procedure that was used for mixing specimens with aqueous SDS solution:

6. 150 g of beach sand were added to a 2 in by 4 in testing cylinder.

7. The appropriate volume of SDS solution was added to each cylinder, and the SDS/soil was mixed thoroughly using a spatula.
8. The appropriate volume of CaCl_2 solution was added to each cylinder.
9. Each cylinder was mixed thoroughly using a spatula.
10. Once all constituents had been thoroughly mixed, the top of each cylinder was screeded.

In each case, after preparation, each cylinder was placed in a drying oven and left uncovered for a minimum of 48 hours. Figure 2-2 shows a photograph of the cylinders in the oven used for this research.



Figure 2-2. Cylinders in drying oven

After 48 hours, the dried cylinders were extracted using a Dremel[®] and prepared for UCS testing.

2.4.3 UCS Testing Procedure

UCS testing conformed to guidelines from ASTM D2166 (ASTM 2016). An ELE International Hand Operated Unconfined Compression Tester, Model 25-3602 was used throughout this study (Figure 2-3):

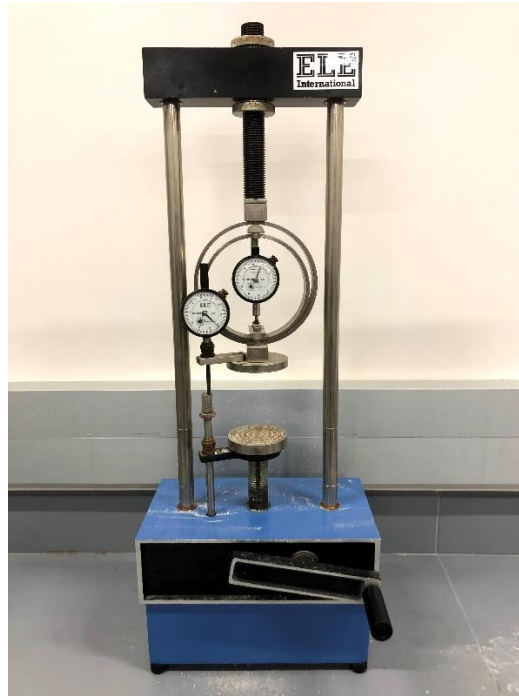


Figure 2-3. ELE International Hand Operated Unconfined Compression Tester, Model 25-3602.

After extraction, each cylinder was transferred to the UCS testing apparatus and its initial length was measured prior to testing. As per the manufacturer's instructions, the hand crank on the UCS apparatus was used to apply compressive loads at a strain rate 2% strain per minute. The load dial and strain dial were recorded at regular intervals until failure. After failure, stress was plotted as a function of strain. Figure 2-4 shows a photograph of a specimen being subjected to UCS testing:

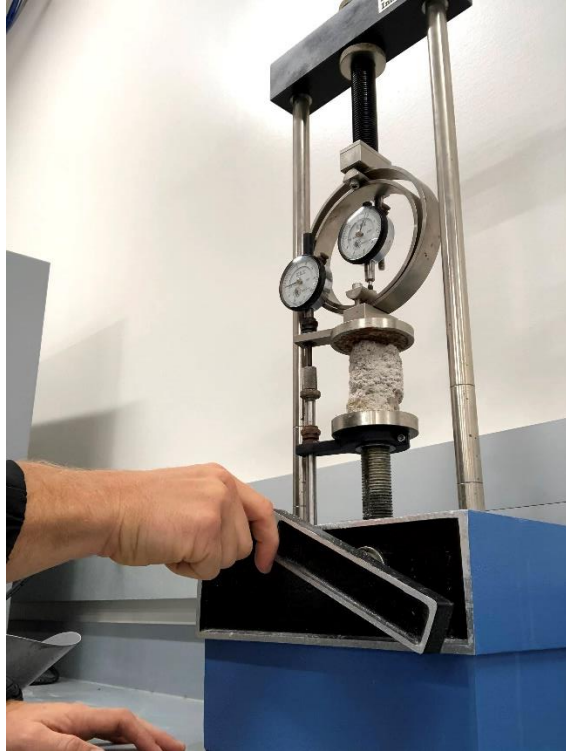


Figure 2-4. UCS testing in progress

UCS was an excellent small-scale laboratory test to quantify the strength of an improved soil sample. Investigators for this study also desired a proof of concept for field applications. The following testing series was designed to use treatment methods that would closely resemble what could be used in the field.

2.5 Sandbox Testing

Two rounds of sandbox testing were conducted. Each sandbox test-series utilized SDS in 20% aqueous solution form. The first round of testing utilized the 2:1 molar ratio between SDS and CaCl_2 . Results from this test-series (see Chapter 3, below) appeared to suggest that more liquid was required to transport the calcium deeper into each box. As such, the second test-series focused upon using a more dilute 0.5 M CaCl_2 solution. In addition, a third series of control tests were conducted whereby either SDS or CaCl_2 alone were added to each sandbox. The following describes details associated with each sandbox test-series:

2.5.1 Sandbox Preparation

Several wooden boxes (5.5 in by 5.5 in by 5.5 in) were constructed using nominal 2x6 lumber. Each box's total volume was approximately 7,300 cc. Based upon the porosity of 0.36, each box could fit approximately 10,850 g of sand with associated *PVs* of approximately 1,930 cc. Premium landscape fabric was secured to the bottom of each box to allow fluid to drain through the sandboxes during treatment. Sand was uniformly added to each box using air pluviation to produce similar relative densities.

Each sandbox testing matrix was designed so that the maximum *PV* filled with SISS constituents did not exceed 100% of the total *PV* because anything over 100% of the total *PV* simply would have drained from the bottom of each sandbox. Eq. 2-5 through Eq. 2-9 were used to compute the appropriate volume of each SISS constituent. Results of this computation are presented below in Table 2-4 and Table 2-5. As mentioned above, a control testing matrix was developed as well. Volumes of SDS and CaCl_2 solution associated with these control tests is presented below in Table 2-6.

Table 2-4. Specifications for mixing constituents for Round One of box testing using SDS as a 20% solution and CaCl₂ as a 2.5M solution.

% of PV Filled by SDS	% of PV Filled	Mass of SDS Powder (g)	V 20% SDS Solution (cc)	Mass of CaCl ₂ Powder (g)	V CaCl ₂ - 2.5M Solution (cc)
15.50%	89%	302.53	1512.64	58.21	209.82
16.00%	92%	312.29	1561.43	60.09	216.59
16.50%	95%	322.05	1610.23	61.97	223.35
17.00%	98%	331.80	1659.02	63.85	230.12
17.50%	101%	341.56	1707.82	65.73	236.89

Table 2-5. Specifications for mixing constituents for Round Two of box testing using SDS as a 20% solution and CaCl₂ as a 0.5M solution.

% of PV Filled by SDS	% of PV Filled	Mass of SDS Powder (g)	V 20% SDS Solution (cc)	Mass of CaCl ₂ Powder (g)	V CaCl ₂ 0.5M solution (cc)
9.75%	83%	190.30	951.50	36.62	659.91
10.25%	88%	200.06	1000.29	38.50	693.75
10.75%	92%	209.82	1049.09	40.37	727.59
11.25%	96%	219.58	1097.88	42.25	761.44
11.75%	100%	229.34	1146.68	44.13	795.28

Table 2-6. Specifications for mixing constituents for Control box testing using SDS as a 20% solution and CaCl₂ as a 2.5M solution.

% of PV Filled by SDS	% of PV Filled	Mass of SDS Powder (g)	V 20% SDS Solution (cc)	Mass of CaCl ₂ Powder (g)	V CaCl ₂ 0.5M solution (cc)
0.00%	100.00%	0.00	0.00	536.16	1932.47
9.75%	49.24%	190.30	951.50	0.00	0.00
10.75%	54.29%	209.82	1049.09	0.00	0.00
11.75%	59.34%	229.34	1146.68	0.00	0.00
19.80%	100.00%	386.49	1932.47	0.00	0.00

2.5.2 Sandbox Treatment Procedure

Once each box had been prepared, the SISS constituents were added to each box surface from a height of 4 in. First, the SDS solution was applied to each box using a handheld watering can. Then, the CaCl_2 was added. Volumes associated with each application are shown above in Table 2-4 through Table 2-6. Since in many cases the CaCl_2 represented a relatively small amount of liquid, a colander was used to ensure even distribution. Photographs of this treatment procedure are presented in Fig. 2-5:



Figure 2-5. Photograph showing sandbox SDS application (Top left), CaCl_2 (Top right), and (Bottom) the sandboxes immediately following treatment.

After treatment, the boxes were allowed to cure for several days. Throughout curing, they were subjected to pocket penetrometer testing. After curing, traction testing was conducted.

2.5.3 Pocket Penetrometer Testing

Pocket penetrometer testing allows the user to quickly estimate the strength of a given soil at various locations along its surface. While it is less accurate than UCS testing, it allows for a quick estimation of surface strength. There is not currently an ASTM standard for pocket penetrometer testing. The testing procedure used in this study involved pressing the tip of a pocket penetrometer into the soil and reading the gauge alongside the penetrometer. This study utilized a Gilson Soil, HM 500 Pocket Penetrometer throughout. A photograph of this instrument is presented below in Fig. 2-6 and 2-7:



Figure 2-6. Photo of the pocket penetrometer used for this study.



Figure 2-7. Photo of compressive strength testing being conducted using pocket penetrometer.

Ideally, pocket penetrometer readings would have been taken daily or every two to three days. However, each penetrometer reading leaves a small puncture hole in the surface of the sand. Individually, these punctures did not appear to affect the overall surface strength of the sand box. But, if too many were placed in a small area, investigators feared that the treated sand would break apart and compromise the results. Therefore, penetrometer testing was limited to three recordings for each box: 2 hours, 2 days and 10 days for the first round of testing, and 2 hours, 2 days and 21 days for the second and control rounds of testing. During each testing event, tests were repeated 4 times for each box.

2.5.4 Traction testing

The most prevalent effects of the wheel-terrain interface are wheel slip and sinkage. (Reina et al 2006). Sinkage is due to plastic flow of the soil under the imposed stresses and can be related to the shear strength of the soil and the characteristics of

the vehicle (Evans 1964). Slip is the relative motion between the tire and the contact surface. As slip increases, the sinkage, and thus the resistance to motion will also increase. This phenomenon is known as the slip sinkage effect (Lyasko 2010). As such there are two main soil strength parameters influencing traction of a wheeled vehicle: compressive strength and shear strength. Adequate compressive strength ensures the terrain will support the weight of the vehicle. Adequate shear strength ensures the vehicle can produce enough tractive effort to overcome the rolling resistance of the terrain. This wheel soil interaction is shown in Figure 2-8.

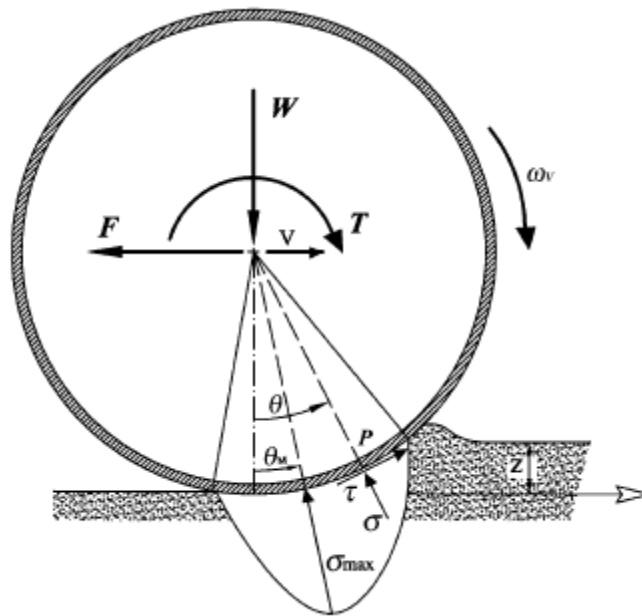


Figure 2-8. Wheel soil interaction model (Reina et al 2006).

The maximum tractive effort that can be developed by a wheel is determined by the shear strength of the terrain according to the Coulomb–Mohr soil failure criterion (Equation 2.12, Reina et al, 2006).

$$F_{\text{max}} = A\tau = A(c + \sigma \tan \phi) = Ac + W \tan \phi \quad (2-10)$$

in which τ is the shear strength of the terrain; c is the cohesion; ϕ is the internal friction angle; A is the wheel contact patch, which is a function of wheel geometry and of the

vertical load acting on the wheel; σ is the normal component of the stress region at the wheel–terrain interface; and W is the vertical load acting on the wheel.

Investigators were able to quantify the compressive strength of soil using the UCS and pocket penetrometer testing. Shear strength testing was not within the scope of this research. Instead, investigators first wanted to qualitatively examine traction holistically. As such a makeshift single wheel traction testing machine was developed as shown below in Fig. 2-9:

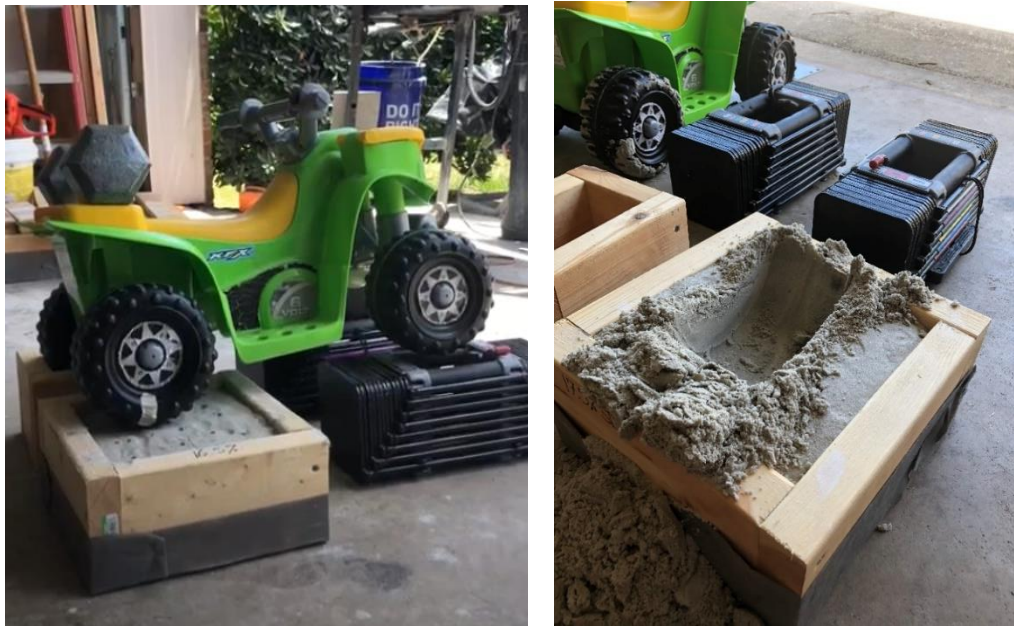


Figure 2-9. (Left) Photo of the single wheel traction tester prepared for testing. (Right) Photo showing the rut caused by traction testing.

This apparatus was a stationary device designed to measure sinkage of a wheel in a state of constant slip. This device was used to measure the maximum rut depth, time to maximum rut depth and rate of sinkage. The testing vehicle used was a Power Wheels® Lil KFX, 6-volt battery powered all-terrain vehicle (ATV). The goal was to add weight to the testing vehicle to mimic the vertical force of a HMMWV. However, this would require 176 lb. be added to the testing wheel and due to the limitations of the

ATV, only 20 lb. were able to be added. The properties of the testing vehicle and HMMWV are shown in Table 2-7 and Table 2-8:

Table 2-7. Properties of the single wheel traction testing vehicle

Gross Weight	13	lbs
Weight on testing tire (measured)	4	lbs
Tire Diameter	7.25	in
Tire Width	4	in
Tire-soil Contact Length	0.90	in
Tire-soil Contact Surface Area	3.6	in ²
Additional weight required to reach 50psi	176.3	lb
Additional weight actually added	20	lb
Resulting psi from added weight	6.7	psi
Max wheel speed	66	rpm
Angular velocity	5.71	rad/s

Table 2-8. Properties of a High Mobility Multipurpose Wheeled Vehicle (HMMWV).

Gross Weight	11500	lbs
Tire Diameter	37	in
Tire Width	12.5	in
Weight per tire (equal distribution)	2875	lbs
Tire pressure (max load)	50	psi
Tire-soil Contact area	57.5	in ²
Tire-soil Contact length	4.6	in

2.5.5 Crust Depth Testing

Following the pocket penetrometer and traction tests, the effective treatment depth was estimated. Investigators noticed during the first round of box testing that the treatment formed a hardened crust upon the soil surface. As a result of the traction test, a rut hole was formed exposing the depth of this crust. This rut hole can be seen in Figure 2-9. The thickness of the hardened surface layer was measured using a standard tape measure (Figure 2-10) and this value was used as an estimate for effective treatment depth.



Figure 2-10. Photo showing the top crust formed as a result of SISS treatment in a sandbox.

2.6 Dissolution Testing

The final test-series was aimed at determining the rate and extent to which the improved soil dissolves or deteriorates in sea water – a critical aspect of this treatment if it is to be used as a temporary stabilization measure for naval field exercises.

2.6.1 Specimen Preparation

Specimens were prepared using the same procedures outlined in Section 2.4.1 and Section 2.5.1 in the sense that several cylinders were prepared using mixing and several sandboxes were prepared using the surface percolation technique. Volumetric SISS constituent quantities for each of these tests is presented below in Table 2-9:

Table 2-9. Dissolution Testing Matrix

Test #	Treatment Type	Drying info	% of PV filled by SDS (20% solution)	% of PV filled by CaCl ₂ (0.5M solution)
D-1	Cylinder	Oven: 2 days	11.75%	1.23%
D-2	Cylinder	Oven: 2 days	10.75%	1.13%
D-3	Cylinder	Oven: 2 days	9.75%	1.02%
D-4	Cylinder	Oven: 2 days	19.80%	0.00%
D-5	Sandbox	Open air: 7 days	11.75%	1.23%
D-6	Sandbox	Open air: 7 days	10.75%	1.13%
D-7	Sandbox	Open air: 7 days	9.75%	1.02%
D-8	Sandbox	Open air: 21 days	11.75%	0.00%
D-9	Sandbox	Open air: 21 days	10.75%	0.00%
D-10	Sandbox	Open air: 21 days	9.75%	0.00%

2.6.2 Testing Procedure

Cylinder dissolution testing was performed by submerging treated cylinders in 1,200 mL of seawater obtained from Atlantic Beach, FL. In addition, control tests were conducted whereby cylinders were submerged in 1,200 mL of distilled water. Sandbox dissolution testing consisted of obtaining a portion of hardened crust from the sandbox surface and submerging it in either distilled water or saltwater. In both cases (sandbox or cylinder) observations were then taken to determine how long it took each sample to dissolve. The specimen was considered “dissolved” when it had lost its stabilized structure and disorganized into a pile of sand. Note that tests D-5 through D-7 were only given 7 days to dry due to time constraints. Ideally these would have been given 21 days to dry. Note as well that constituent levels were chosen to match Round 2 of sand box testing. An example of dissolution testing is shown below in Fig. 2-11:

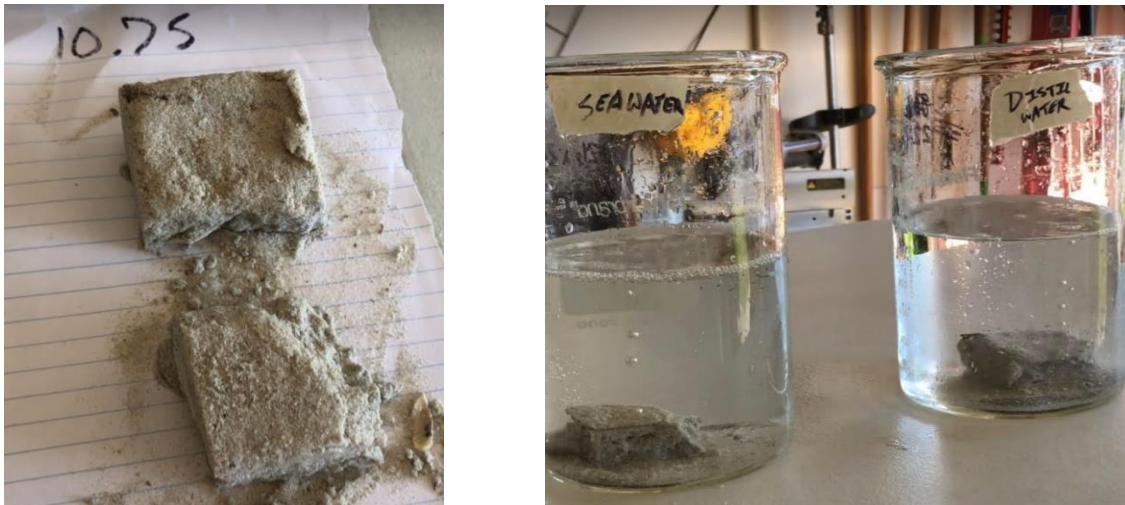


Figure 2-11. (Left) Photo of the specimens cut out of the sand box treated with 10.75% of the PV filled with SDS for test D-6. (Right) Photo showing the side-by-side dissolution testing of test D-6.

CHAPTER 3
RESULTS

3.1 Unconfined Compression Test Results

Combined results from cylinder testing are presented below in tabular form in

Table 3-1 and in graphical form in Figure 3-1:

Table 3-1. Consolidated Results of UCS Testing

Powder Round 1			Powder Round 2			Solution		
Test #	% PV filled by SDS	Strength (psi)	Test #	% of PV filled by SDS	Strength (psi)	Test #	% PV filled by SDS	Strength (psi)
UCTP1-1	14.15%	0.00	UCTP2-1	27.80%	87.29	UCTS-1	4.19%	0.00
UCTP1-2	28.31%	22.30	UCTP2-2	36.14%	39.87	UCTS-2	8.37%	14.00
UCTP1-3	42.46%	0.00	UCTP2-3	44.48%	34.52	UCTS-3	12.56%	0.00
UCTP1-4	56.61%	27.47	UCTP2-4	52.82%	42.34	UCTS-4	16.74%	0.00
UCTP1-5	70.76%	59.46	UCTP2-5	61.16%	68.75	UCTS-5	20.93%	21.91
UCTP1-6	84.92%	45.05	UCTP2-6	69.50%	62.16	UCTS-6	25.11%	16.24
UCTP1-7	99.07%	0.00	UCTP2-7	77.84%	42.68	UCTS-7	29.30%	5.97
UCTP1-8	113.22%	0.00	UCTP2-8	86.18%	43.34	UCTS-8	33.48%	0.00
UCTP1-9	127.37%	0.00	UCTP2-9	94.52%	52.88	UCTS-9	37.67%	37.22
UCTP1-10	141.53%	0.00	UCTP2-10	102.86%	46.20	UCTS-10	41.85%	3.61
			UCTP2-11	111.20%	31.10			

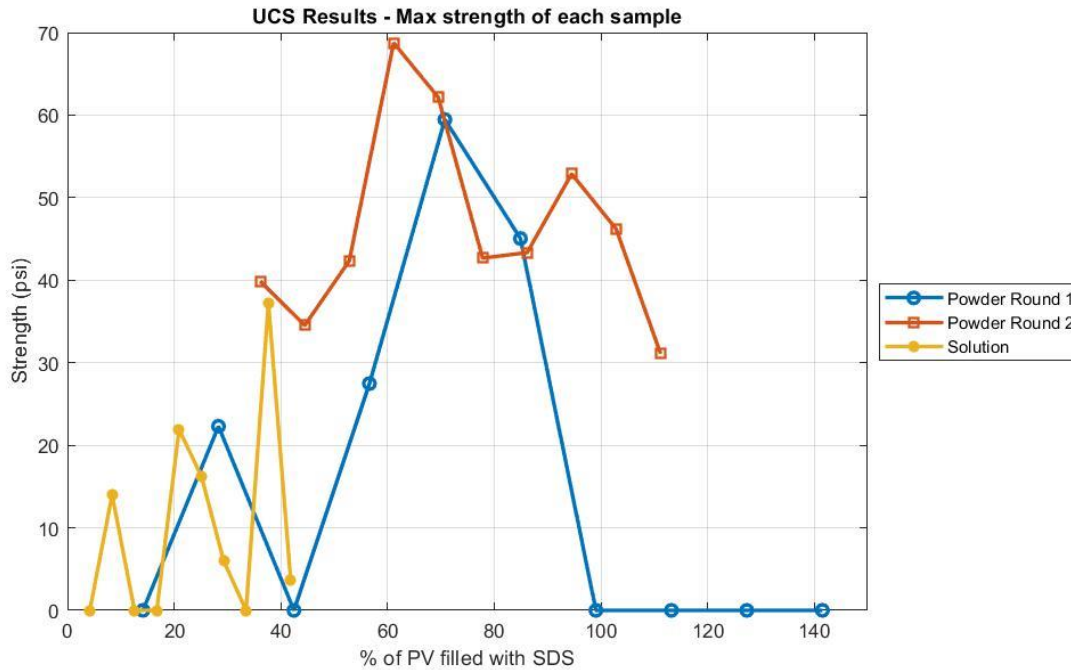


Figure 3-1. Plot summary of UCS Results (note – results from UCTP2-1 removed as an outlier)

As shown in Fig. 3-1, results suggest that optimal strength is achieved when approximately 80% of the PV is filled with SDS powder. In addition, results appear to suggest that similar strengths were achieved for a given SDS percentage (assuming stoichiometric balance) for both aqueous and powder SDS. As such, a combined plot was developed that included all data points from cylinder testing (note that UCTP2-1 was omitted as an outlier). A best-fit regression curve was fit through these data of the form $y = ax^2 + bx + c$ as shown below in Fig. 3-2:

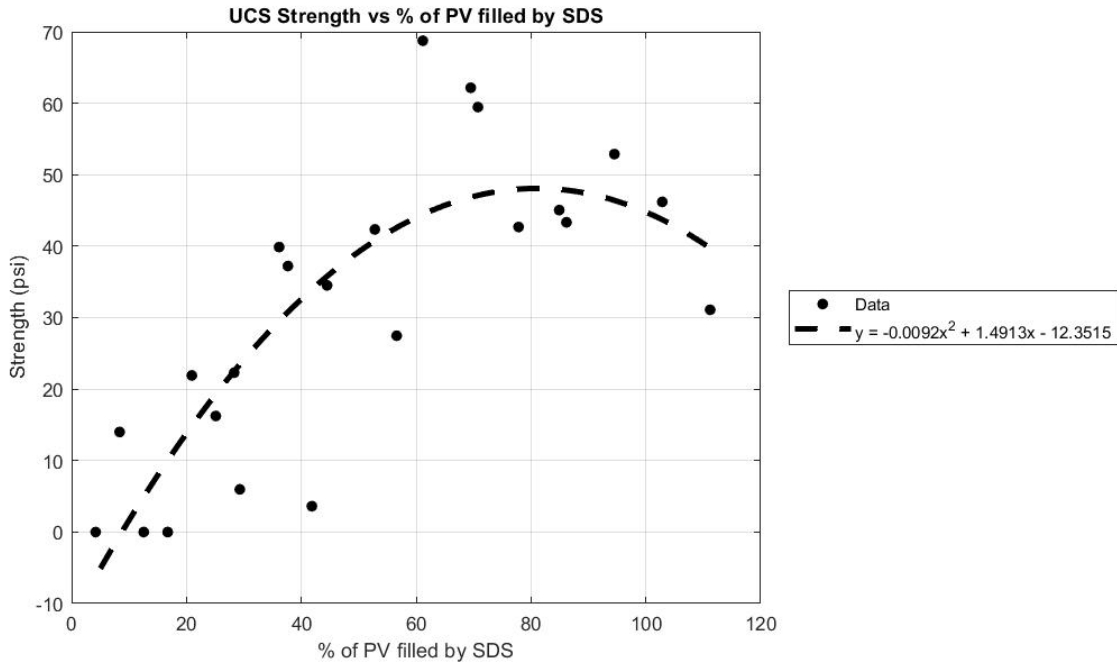


Figure 3-2. Best fit curve of UCS Results. Note: Regression only applies within the bounds of the dataset.

As shown, the resulting maximum compressive strength was 48.4 psi which occurred at 81.4% of the PV filled with SDS. Unfortunately, as shown in Fig. 3-1, this maximum is well beyond what can be feasibly achieved using SDS in aqueous solution form. Thus, while surface percolation may produce some strength improvements, these preliminary data suggested that results from sandbox testing would be modest.

3.2 Sand Box Results

3.2.1 Pocket Penetrometer Testing

Results from pocket penetrometer testing are presented below. Table 3-2 and Figure 3-3 present the results from the first round of box testing, Table 3-3 and Figure 3-4 present the results from the second round of box testing. Table 3-4 and Figure 3-5 present the results of the control box testing.

Table 3-2. Pocket Penetrometer Results (20% SDS solution // 2.5M CaCl₂ solution)

Test #	PP1-1	PP1-2	PP1-3	PP1-4	PP1-5
% of PV with SDS	17.50%	17.00%	16.50%	16.00%	15.50%
Strength after 2 hours (psi)	N/A	N/A	N/A	2.78	2.08
	N/A	N/A	N/A	2.78	2.08
	N/A	N/A	N/A	2.78	2.08
	N/A	N/A	N/A	2.78	2.08
2 hour average	N/A	N/A	N/A	2.78	2.08
2 hour std deviation	N/A	N/A	N/A	0.00	0.00
Strength after 4 days (psi)	9.72	10.42	3.47	5.56	6.95
	11.81	11.81	3.47	6.95	6.95
	11.81	13.89	3.47	17.64	8.47
	13.89	13.89	3.47	24.31	10.42
4 day average	12.50	12.50	3.47	13.61	8.20
4 day std deviation	1.47	1.47	0.00	7.75	1.43
Strength after 10 days (psi)	17.36	10.42	3.47	N/A	N/A
	20.84	13.89	3.47	N/A	N/A
	31.25	17.36	3.47	N/A	N/A
	38.20	27.78	3.47	N/A	N/A
10 day average	26.91	17.36	3.47	N/A	N/A
10 day std deviation	8.28	6.50	0.00	N/A	N/A

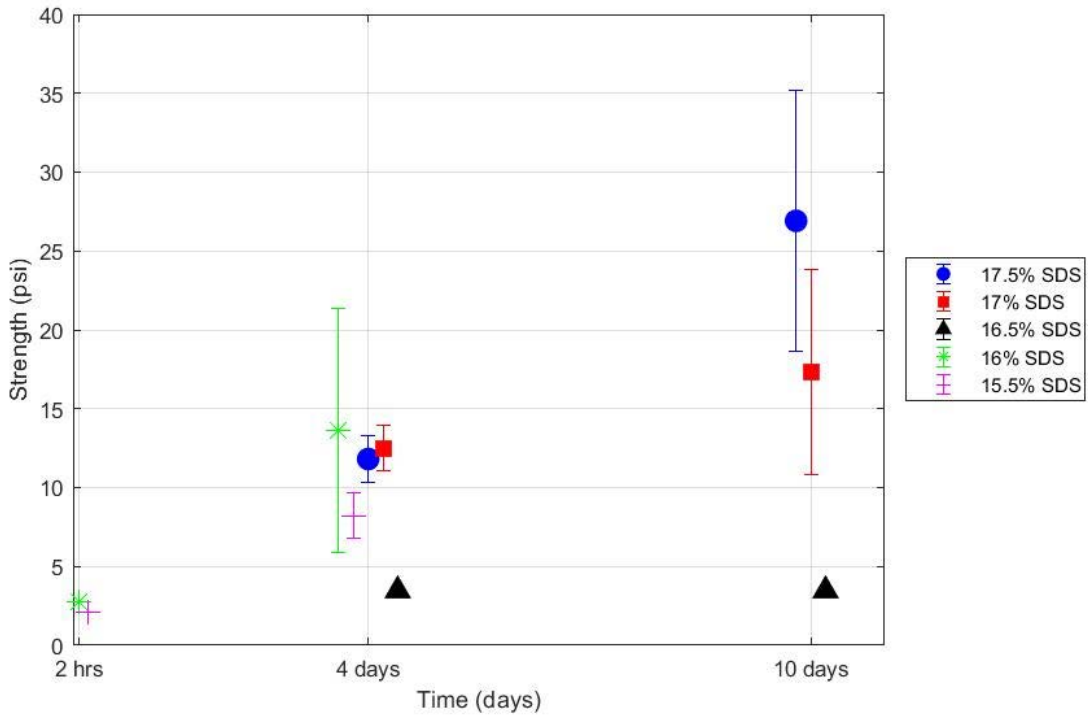


Figure 3-3. Pocket Penetrometer Results (20% SDS solution // 2.5M CaCl₂ solution).
 Note: Symbols denote averages, wings denote standard deviations.

Table 3-3. Pocket Penetrometer Results (20% SDS solution // 0.5M CaCl₂ solution)

Test #	PP2-1	PP2-2	PP2-3	PP2-4	PP2-5
% of PV with SDS	11.75%	11.25%	10.75%	10.25%	9.75%
Strength after 2 hours (psi)	3.47	3.47	3.47	3.47	3.47
	3.47	3.47	3.47	3.47	3.47
	3.47	3.47	3.47	3.47	3.47
	3.47	3.47	3.47	3.47	3.47
2 hour average	3.47	3.47	3.47	3.47	3.47
2 hour std deviation	0.00	0.00	0.00	0.00	0.00
Strength after 2 days (psi)	9.72	10.42	3.47	6.95	3.47
	10.42	10.42	3.47	6.95	3.47
	10.42	10.42	3.47	6.95	3.47
	13.89	10.42	3.47	6.95	3.47
2 day average	11.11	10.42	3.47	6.95	3.47
2 day std deviation	1.63	0.00	0.00	0.00	0.00
Strength after 21 days (psi)	55.56	48.62	3.47	13.89	17.36
	59.03	52.09	16.00	13.89	17.36
	59.03	52.09	41.67	13.89	17.36
	62.51	55.56	41.67	13.89	17.36
21 day average	59.03	52.09	25.70	13.89	17.36
21 day std deviation	2.46	2.46	16.57	0.00	0.00

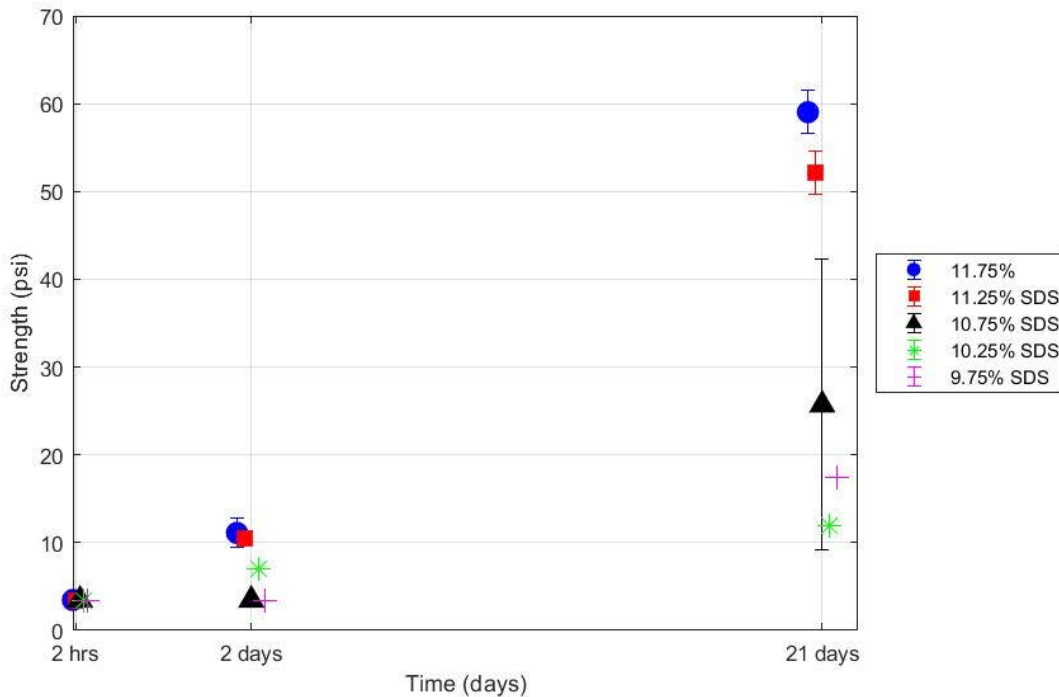


Figure 3-4. Pocket Penetrometer Results (20% SDS solution // 0.5M CaCl₂ solution).

Note: Symbols denote averages, wings denote standard deviations. X-axis not to scale.

Table 3-4. Pocket Penetrometer Results (Control Tests)

Test #	PPC-1	PPC-2	PPC-3	PPC-4	PPC-5	PPC-6
% of PV with SDS	0.00%	0.00%	19.80%	11.75%	10.75%	9.75%
Strength after 2 hours (psi)	0.00	2.08	2.08	8.33	6.95	6.95
	0.00	2.08	2.08	8.33	6.95	6.95
	0.00	2.08	2.08	8.33	6.95	6.95
	0.00	2.08	2.08	8.33	6.95	6.95
2 hour average	0.00	2.08	2.08	8.33	6.95	6.95
2 hour std deviation	0.00	0.00	0.00	0.00	0.00	0
Strength after 4 days (psi)	0.00	2.78	3.47	10.42	11.11	10.42
	0.00	2.78	3.47	10.42	11.11	10.42
	0.00	2.78	3.47	10.42	11.11	10.42
	0.00	2.78	3.47	10.42	11.11	10.42
4 day average	0.00	2.78	3.47	10.42	11.11	10.42
4 day std deviation	0.00	0.00	0.00	0.00	0.00	0
Strength after 10 days (psi)	0.00	2.78	34.73	5.56	62.51	34.73
	0.00	3.47	55.70	6.95	62.51	34.73
	0.00	3.47	62.51	17.64	62.51	44.73
	0.00	6.95	63.34	24.31	62.51	45.84
10 day average	0.00	4.17	54.07	13.61	62.51	40.00
10 day std deviation	0.00	1.63	11.55	7.75	0.00	5.29

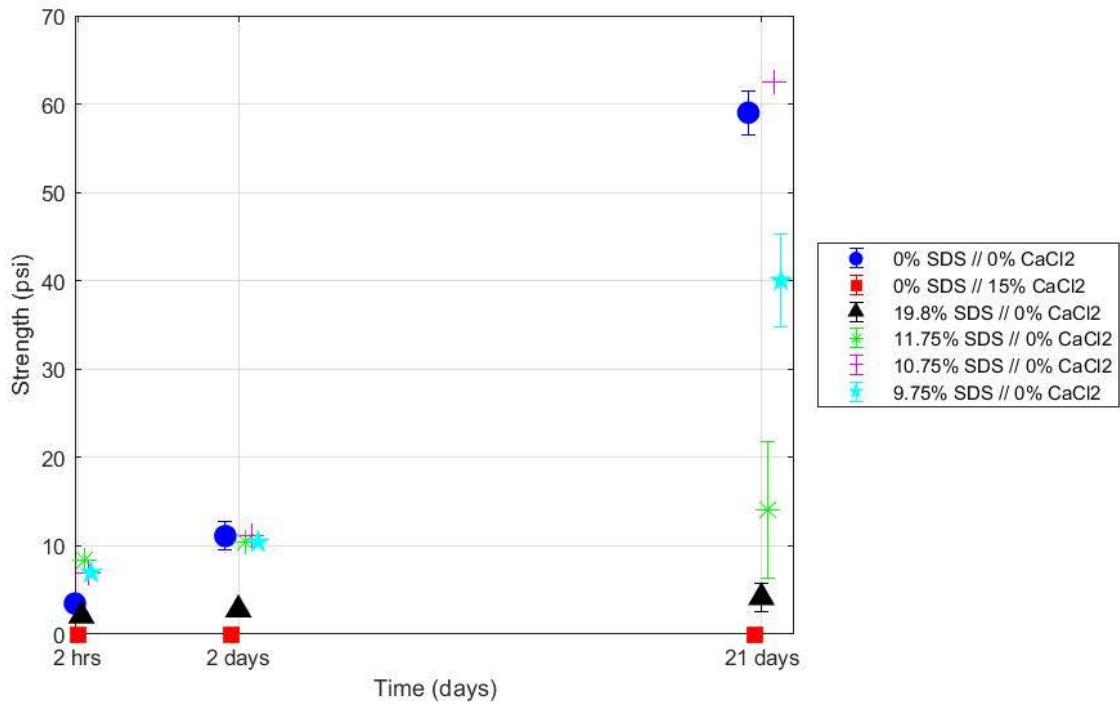


Figure 3-5. Pocket Penetrometer Results (Control Tests). Note: Symbols denote averages, wings denote standard deviations. X-axis not to scale.

3.2.2 Traction

Results from traction testing are presented below in Table 3-5 through Table 3-10. Figures 3-6 through 3-8 display the rate of sinkage with respect to time. To determine the rate of sinkage each traction test was video recorded, and the rut depth was estimated at 10 equally spaced time intervals.

Table 3-5. Max Sinkage (20% SDS solution // 2.5M CaCl₂ solution)

Test #	% of PV filled by SDS	% of PV filled by CaCl ₂	Rut Depth (in)	Time to max rut depth (s)
MS1-1	17.50%	1.84%	3	183
MS1-2	17.00%	1.79%	2.5	164
MS1-3	16.50%	1.73%	3.625	72
MS1-4	16.00%	1.68%	3.625	76
MS1-5	15.50%	1.63%	3.625	47

Table 3-6. Sinkage Rates (20% SDS solution // 2.5M CaCl₂ solution)

17.50%		17.00%		16.50%		16.00%		15.50%	
Time (s)	Rut Depth (in)								
0	0.00	0	0.00	0	0.00	0	0.00	0	0.00
18	0.13	16	0.13	7	0.50	8	0.13	5	0.10
37	0.25	33	0.25	14	0.63	15	0.25	9	0.25
55	0.50	49	0.50	22	1.00	23	0.38	14	0.35
73	0.75	66	0.63	29	1.50	30	0.50	19	0.50
92	1.00	82	0.75	36	2.00	38	1.00	24	0.75
110	1.25	98	1.25	43	2.38	46	1.50	28	1.00
128	1.75	115	1.50	50	2.75	53	1.75	33	2.00
146	2.13	131	2.00	58	3.00	61	2.63	38	2.50
165	2.50	148	2.25	65	3.50	68	3.00	42	3.25
183	3.00	164	2.50	72	3.63	76	3.63	47	3.63

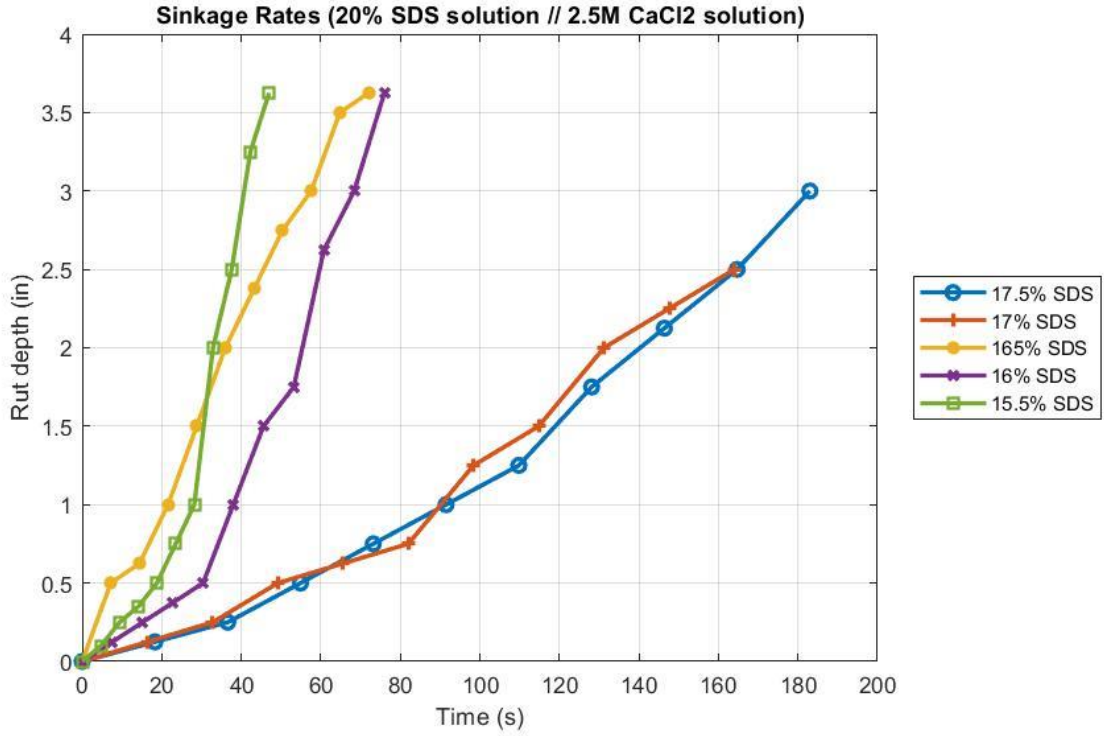


Figure 3-6. Sinkage Rates (20% SDS solution // 2.5M CaCl2 solution)

Table 3-7. Max Sinkage (20% SDS solution // 0.5M CaCl2 solution)

Test #	% of PV filled by SDS	% of PV filled by CaCl2	Rut Depth (in)	Time to max rut depth (s)
MS2-1	11.75%	1.23%	3.625	82
MS2-2	11.25%	1.18%	3.625	60
MS2-3	10.75%	1.13%	3.625	40
MS2-4	10.25%	1.08%	3.625	50
MS2-5	9.75%	1.02%	3.25	50

Table 3-8. Sinkage Rates (20% SDS solution // 0.5M CaCl2 solution)

11.75%		11.25%		10.75%		10.25%		9.75%	
Time (s)	Rut Depth (in)								
0	0.00	0	0.00	0	0.00	0	0.00	0	0.00
8	0.13	6	0.00	4	0.375	5	0.38	5	0.38
16	0.25	12	0.13	8	0.63	10	1.00	10	0.50
25	0.50	18	0.25	12	1.00	15	1.25	15	0.75
33	1.00	24	0.75	16	1.25	20	1.50	20	1.00
41	1.50	30	1.50	20	1.75	25	1.50	25	1.25
49	2.25	36	2.00	24	2.50	30	2.50	30	1.75
57	2.75	42	2.50	28	3.00	35	3.13	35	2.50
66	3.25	48	3.25	32	3.38	40	3.38	40	3.00
74	3.50	54	3.50	36	3.50	45	3.50	45	3.13
82	3.63	60	3.63	40	3.63	50	3.63	50	3.25

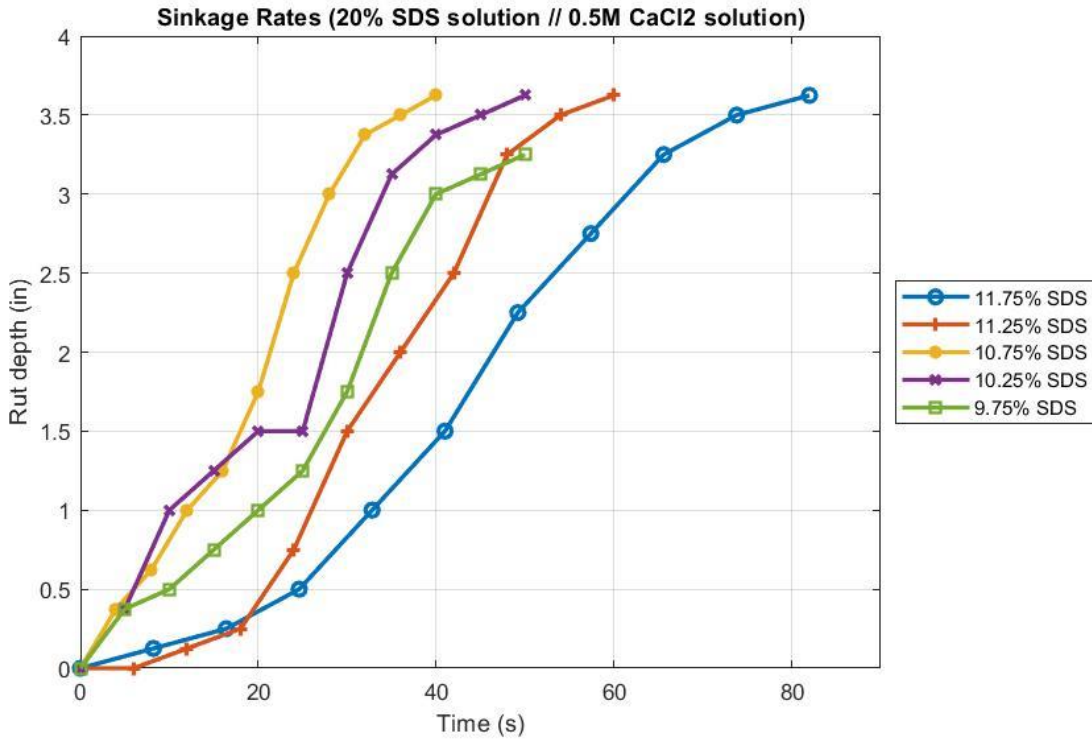


Figure 3-7. Sinkage Rates (20% SDS solution // 0.5M CaCl2 solution)

Table 3-9. Max Sinkage (Control Tests)

Test #	% of PV filled by SDS	% of PV filled by CaCl2	Rut Depth (in)	Time to max rut depth (s)
MSC-1	0.00%	0.00%	3.625	16
MSC-2	0.00%	15.00%	3.625	75
MSC-3	19.80%	0.00%	3.625	200
MSC-4	11.75%	0.00%	Not tested	Not tested
MSC-5	10.75%	0.00%	Not tested	Not tested
MSC-6	9.75%	0.00%	Not tested	Not tested

Table 3-10. Sinkage Rates (Control Tests)

100% SDS // 0% CaCl2		0% SDS // 100% CaCl2		0% SDS // 0% CaCl2	
Time (s)	Rut Depth (in)	Time (s)	Rut Depth (in)	Time (s)	Rut Depth (in)
0	0.00	0	0.00	0	0.00
20	0.13	8	0.63	2	0.75
40	0.25	15	0.75	3	1.00
60	0.38	23	1.00	5	1.50
80	0.50	30	1.25	6	2.00
100	0.75	38	1.25	8	2.50
120	1.25	45	1.38	10	3.00
140	2.25	53	2.00	11	3.25
160	3.13	60	2.50	13	3.38
180	3.50	68	3.25	14	3.50
200	3.63	75	3.63	16	3.63

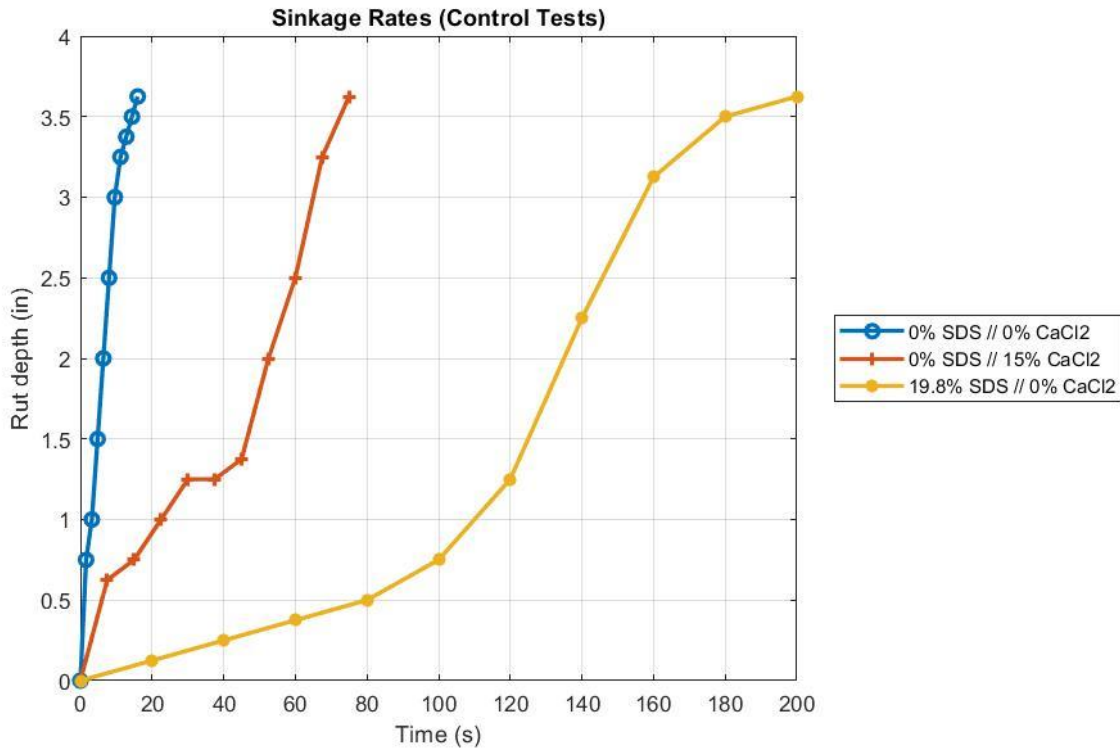


Figure 3-8. Sinkage Rates (Control Tests)

3.2.3 Crust Depth

Results from crust depth testing are presented below in Table 3-11 through Table 3-13. Figure 3-9 and 3-10 present crust depth plotted as a function of %PV with SDS for round two testing (TD2-1 through TD2-5) and the control round of testing (TDC-1 through TDC-6), respectively. Round one results (TD1-1 through TD1-5) were not plotted since only two of the five values were recorded. As shown in Figs. 3-9 and 3-10, best-fit regression lines were fit through the data to develop relationships between crust depth and SDS as a function of % PV.

Table 3-11. Crust Depth (20% SDS solution // 2.5M CaCl₂ solution)

Test #	% of PV filled by SDS	% of PV filled by CaCl ₂	Crust Depth
TD1-1	17.50%	1.84%	1.25
TD1-2	17.00%	1.79%	0.75
TD1-3	16.50%	1.73%	Not measured
TD1-4	16.00%	1.68%	Not measured
TD1-5	15.50%	1.63%	Not measured

Table 3-12. Crust Depth (20% SDS solution // 0.5M CaCl₂ solution)

Test #	% of PV filled by SDS	% of PV filled by CaCl ₂	Crust Depth (in)
TD2-1	11.75%	1.23%	1.38
TD2-2	11.25%	1.18%	1.25
TD2-3	10.75%	1.13%	1.50
TD2-4	10.25%	1.08%	0.75
TD2-5	9.75%	1.02%	0.75

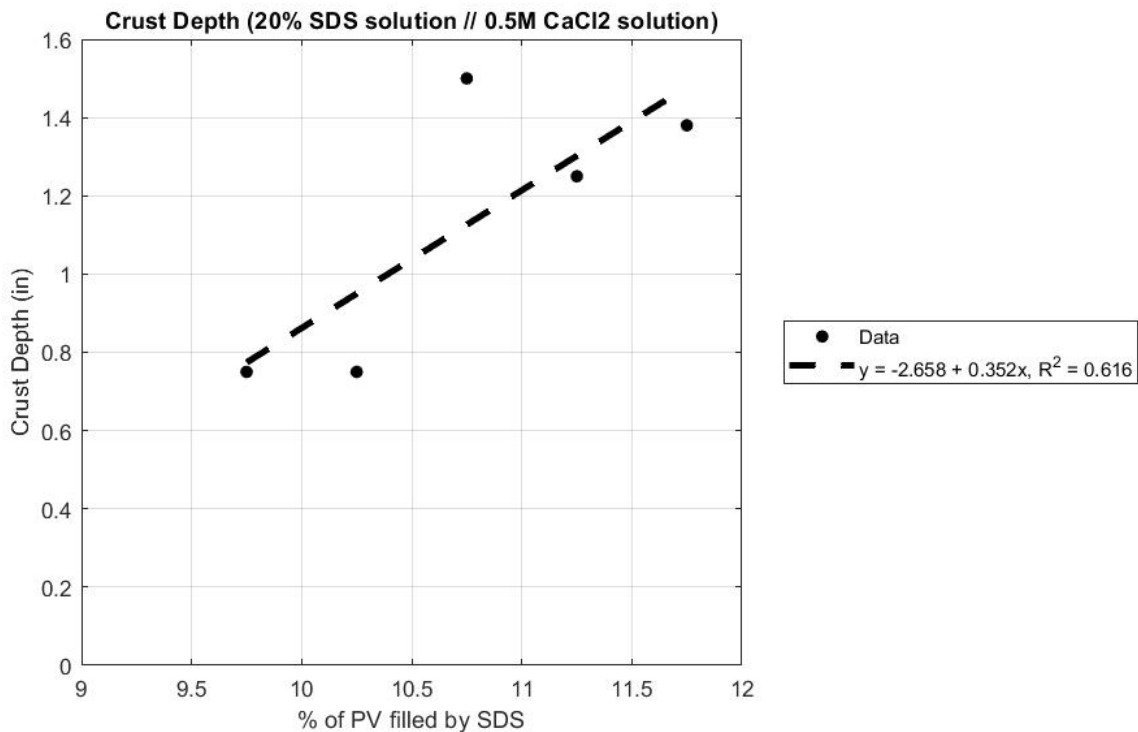


Figure 3-9. Crust Depth Results from Round Two of Testing (20% SDS solution // 0.5M CaCl₂ solution). Note: Regression only applies within the bounds of the dataset.

Table 3-13. Crust Depth (Control Tests)

Test #	% of PV filled by SDS	% of PV filled by CaCl2	Crust Depth (in)
TDC-1	0.00%	0.00%	0.00
TDC-2	0.00%	15.00%	0.00
TDC-3	19.80%	0.00%	1.00
TDC-4	11.75%	0.00%	0.38
TDC-5	10.75%	0.00%	0.88
TDC-6	9.75%	0.00%	0.75

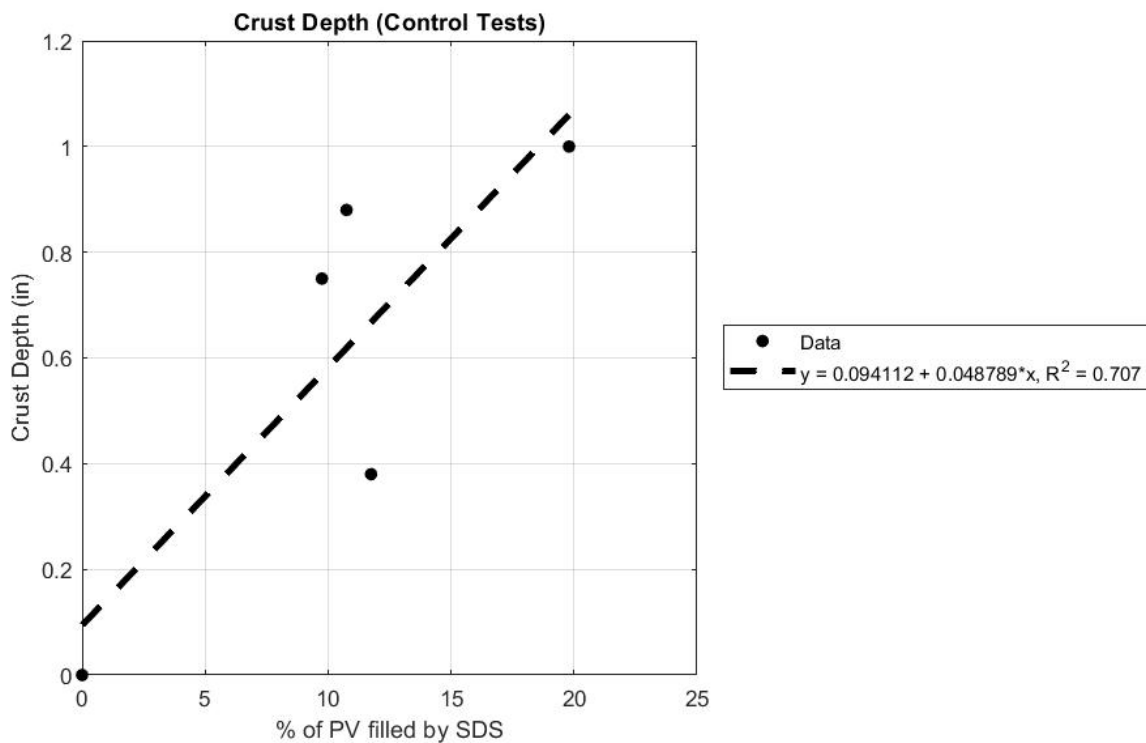


Figure 3-10. Crust Depth Results from Control Testing. Note: Regression only applies within the bounds of the dataset.

3.3 Dissolution

The dissolution testing results are summarized in Table 3-14. The cylinders in tests D-1 through D-4 barely held their structure enough to get them into each jar of water. The specimens in tests D-8 through D-9 were able to be placed on the bottom of each jar before completely dissolving.

Table 3-14. Dissolution Results

Test #	Treatment Type	Drying info	% of PV filled by SDS (20% solution)	% of PV filled by CaCl ₂ (0.5M solution)	Dissolution time in seawater (s)	Dissolution time in distilled water (s)
D-1	Cylinder	Oven: 2 days	11.75%	1.23%	2	2
D-2	Cylinder	Oven: 2 days	10.75%	1.13%	2	2
D-3	Cylinder	Oven: 2 days	9.75%	1.02%	2	3
D-4	Cylinder	Oven: 2 days	19.80%	0.00%	6	2
D-5	Sandbox	Open air: 7 days	11.75%	1.23%	3600	2400
D-6	Sandbox	Open air: 7 days	10.75%	1.13%	840	600
D-7	Sandbox	Open air: 7 days	9.75%	1.02%	2400	1080
D-8	Sandbox	Open air: 21 days	11.75%	0.00%	6	4
D-9	Sandbox	Open air: 21 days	10.75%	0.00%	23	60
D-10	Sandbox	Open air: 21 days	9.75%	0.00%	40	21

CHAPTER 4 DISCUSSION

Results appeared to show that treating beach sand with anionic surfactant increased its strength. Strength improvements were observed when treating the sand with various amounts of each constituent (SDS and CaCl₂) using two different application methods – both mixing and percolation. This chapter analyzes the results from the test-series associated with each treatment method. Following data analysis is a discussion regarding upscaling for field applications.

4.1 Data Analysis – Strength Testing

Results from the UCS testing indicated that when beach sand is treated in a cylinder with SDS and CaCl₂ (stoichiometrically balanced using a 2:1 chemical ratio) a parabolic relationship exists between UCS and % of PV filled with SDS that appears to indicate a local maximum of 48 psi that corresponds to approximately 81.4% of the PV filled with SDS. While higher UCS results were achieved when using SDS in powder versus 20% aqueous solution, it is likely that these higher strengths are a result of higher levels of SDS, and not simply the fact that the SDS was in powder form.

Results from the bench-scale sandbox testing showed that comparable strength improvements could be achieved when compared to cylinder testing using significantly lower quantities of SDS and CaCl₂. This is illustrated below in Table 4-1:

Table 4-1. Maximum Average Compressive Strength Results from each testing series

Treatment Method	% of PV filled with SDS	SDS Form	CaCl ₂ Form	Constituent Ratio (SDS/CaCl ₂)	Drying Method	Drying Time (days)	Testing method	Strength (psi)
Cylinder (mixing)	81.4%	Powder	2.5M Solution	5.2	Oven	2	UCS (best fit curve)	48.4
Sandbox (percolation)	17.5%	20% Solution	2.5M Solution	5.2	Open Air	10	Pocket Penetrometer (average)	26.91
Sandbox (percolation)	11.75%	20% Solution	0.5M Solution	5.2	Open Air	21	Pocket Penetrometer (average)	59.03
Sandbox (percolation)	10.75%	20% Solution	N/A	0.0	Open Air	21	Pocket Penetrometer (average)	62.5
Sandbox (percolation)	19.8%	20% Solution	N/A	SDS alone	Open Air	21	Pocket Penetrometer (average)	54.07
Sandbox (percolation)	0%	N/A	0.5M Solution	CaCl ₂ alone	Open Air	21	Pocket Penetrometer (average)	4.17

To generate Table 4-1, maximum strength data from Chapter 3 were averaged.

These results along with dissolution results appear to show a number of interesting mechanisms related to soil strength. First, control testing shows that treatment with calcium chloride alone does little to improve soil strength. Control testing with SDS shows that treatment with SDS alone may increase soil strength. However, dissolution testing with SDS-only control specimens shows that this apparent increase in soil strength may largely be due to reprecipitated SDS. SDS is highly soluble and the specimens treated with SDS only dissolved very quickly. Another possible explanation is that the dodecyl sulfate tails from the SDS may have bonded directly to the quartz sand particles (since quartz is a dipolar molecule like water). But the end result is largely the same in the sense that whatever complex was formed using SDS alone quickly deteriorated in water. One focus of future work will be to conduct a series of

tests using “clean” Ottawa sand to determine which of these mechanisms is most likely (although as noted, the point may be moot). In particular, scanning electron microscopy (SEM) and x-ray diffraction (XRD) analyses will be conducted to better determine the mechanisms associated with the observed strength improvements.

On the other hand, specimens that were treated with both SDS and calcium chloride also achieved higher surface strengths and strength tended increase with increasing levels of SDS (Fig. 4-1). Additionally, dissolution testing with these specimens showed that they were relatively less soluble when compared to specimens treated with SDS only. Taken together, these data would appear to indicate that the SISS mechanism is functioning as designed in the sense that the calcium ions from the calcium chloride are bonding to the SDS' dodecyl sulfate tails. And, reprecipitated calcium chloride salt is doing little to improve soil strength. Again, future work will focus on characterizing this apparent calcium dodecyl sulfate complex more definitively using SEM/XRD testing.

It is also interesting to note that dry time also played an apparent role in strength improvement. Data showed that as dry time increased, the compressive strength consistently improved. However, there was significant variability observed in the data, and this appears to be a function of SDS quantity and dry time. To illustrate this, Fig. 4-2 through 4-4 (below) were generated by plotting the standard deviation of the penetrometer results at each time step for each SDS quantity. As shown the standard deviation tended to increase with increasing SDS quantity and dry time. This relationship between variability, SDS quantity, and dry time is strongest in the control tests when no CaCl_2 was added (Figure 4-4). In other words, variability decreased when

CaCl₂ was introduced. These data may suggest that there was insufficient calcium to fully react with the SDS. In other words, while SDS and calcium chloride were stoichiometrically balanced, the variability in the data may suggest that the SDS mixed with the soil more effectively than the calcium chloride solution. And, as such, there were insufficient calcium ions to drive the dodecyl sulfate-calcium-dodecyl sulfate reaction over a large area within the soil matrices. Another focus of future work will be to use higher concentration calcium chloride solutions to see if that drives a more robust (in terms of area) reaction within the soils.

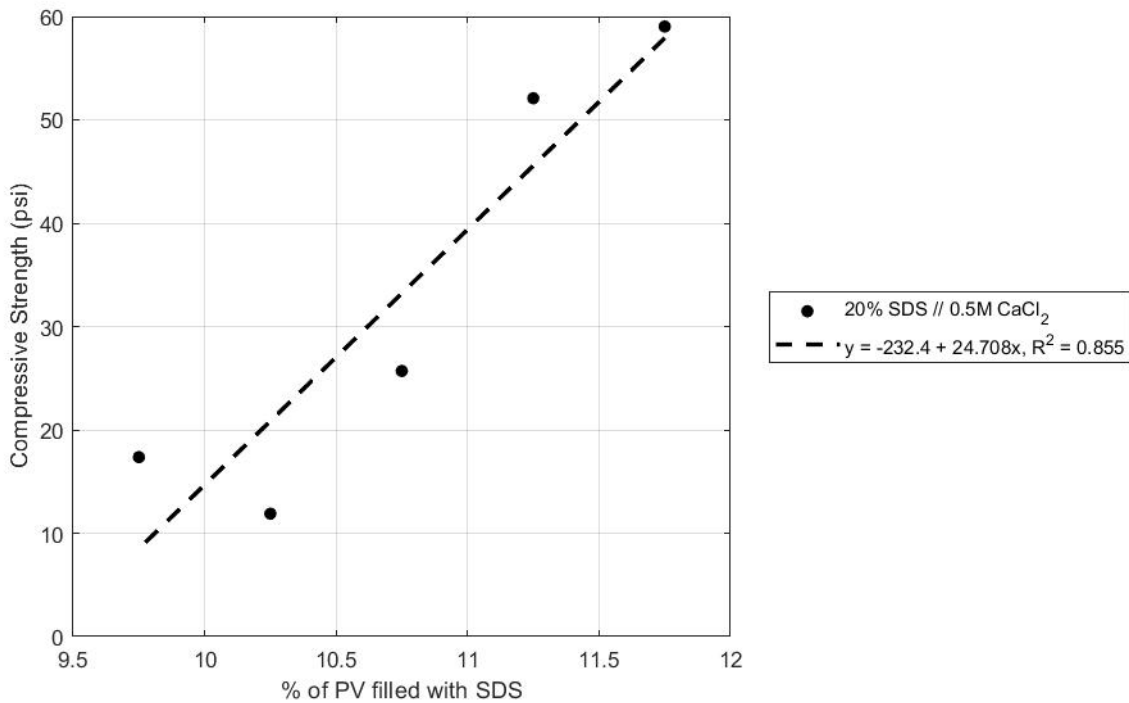


Figure 4-1. Plot of compressive strength vs SDS quantity for sandbox testing Round 2 (20% SDS // 0.5M CaCl₂). Note: Compressive strength values are 21 day averages from penetrometer testing. Regression only applies within the bounds of the dataset.

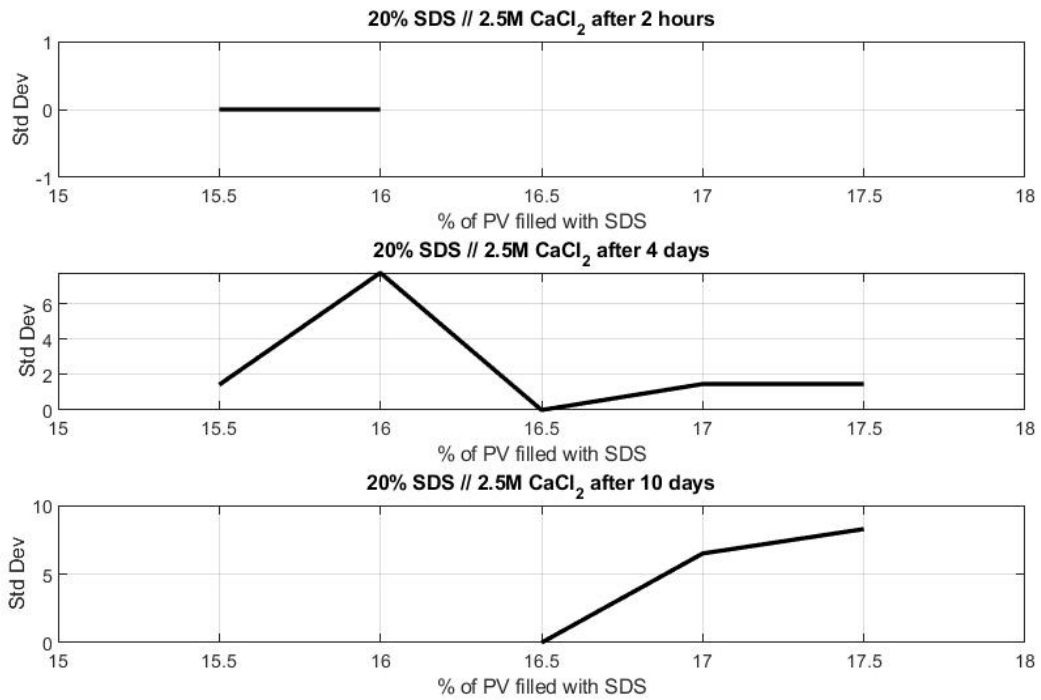


Figure 4-2. Plots of penetrometer results from Round 1 of sandbox testing (20% SDS solution // 2.5M CaCl₂ solution). Standard deviation as a function of SDS quantity.

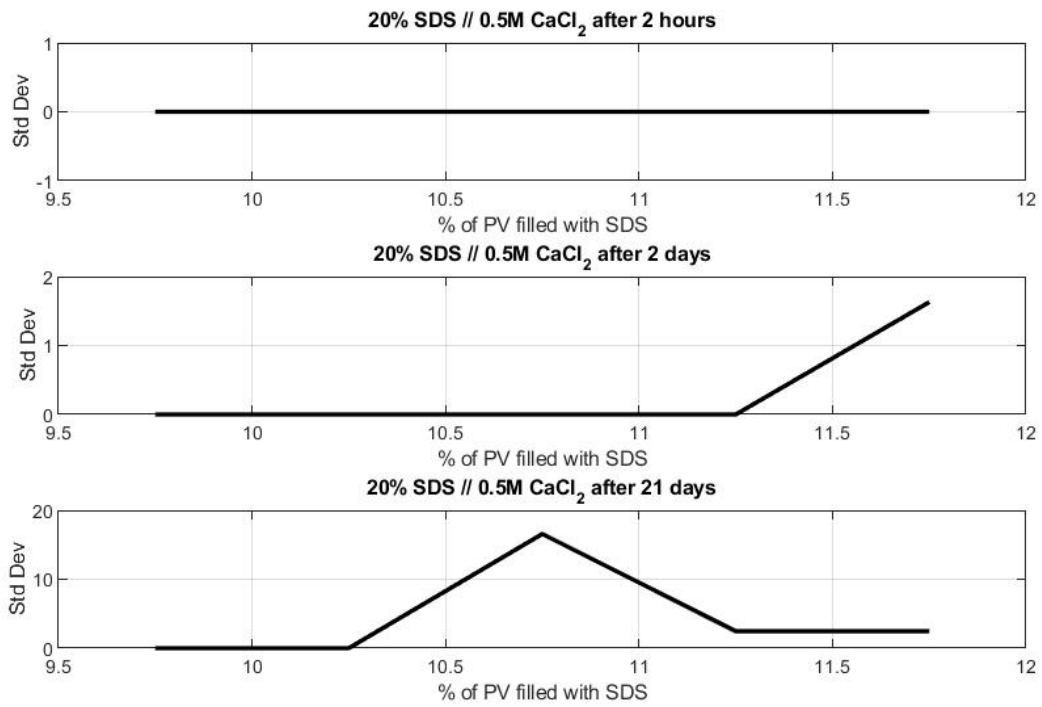


Figure 4-3. Plots of penetrometer results from Round 2 of sandbox testing (20% SDS solution // 0.5M CaCl₂ solution). Standard deviation as a function of SDS quantity.

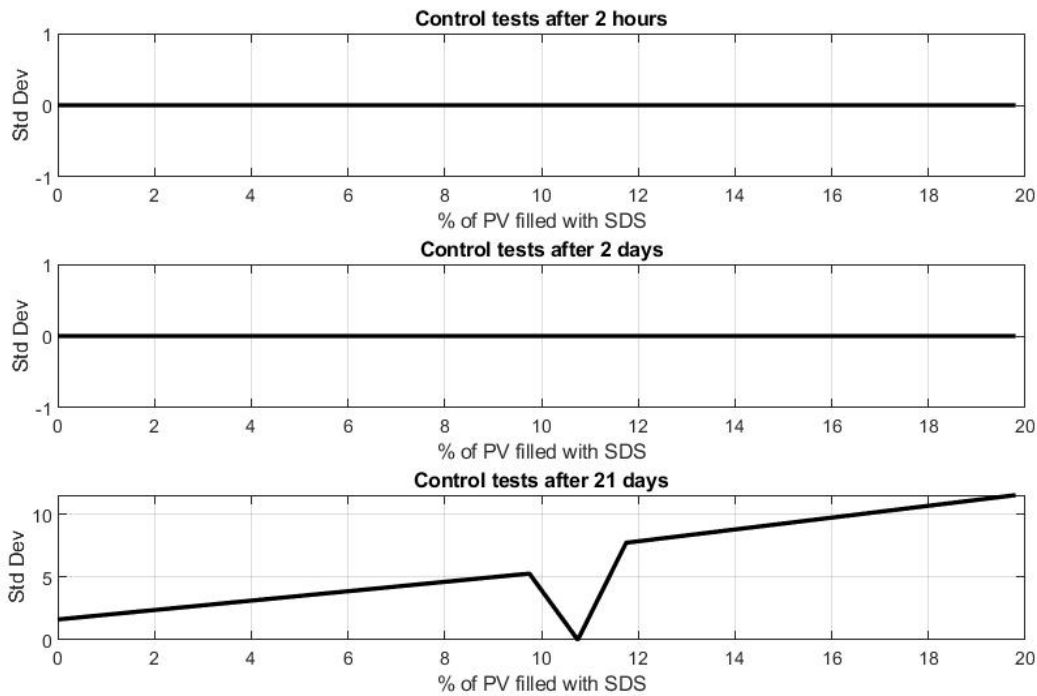


Figure 4-4. Plots of penetrometer results from Control sandbox testing. Standard deviation as a function of SDS quantity.

4.2 Data Analysis – Traction Testing

Results from traction testing showed a positive relationship between the % of PV filled with SDS and the time it took for the traction tester to reach the maximum rut depth. Since the traction testing machine was a battery-powered Power Wheels® vehicle, researchers suspect that variations exist in the results due to how well the battery was charged at the time of testing. Despite this, it should still be possible to compare results on a test-by-test basis. As shown below in Figure 4-5, time to maximum rut depth was plotted as a function of SDS quantity. Since the max rut depth varied between the tests, the sinkage rates could be estimated by plotting best-fit regression lines through the data in Section 3.2.2 and taking their slopes (Tables 4-2

and 4-3). These slopes were plotted as a function of SDS quantity and compressive strength, respectively (Fig. 4-6 and Fig. 4-7).

Figure 4-5 shows a strong positive relationship between the time it took the traction tester to reach the maximum rut depth (max sinkage) and the SDS quantity. Similarly, Figure 4-6 shows a strong negative relationship between the sinkage rate and the SDS quantity. Each of the figures appear to indicate that the soil becomes more resistive to wheeled vehicle sinkage as the amount of SDS added to the soil is increased. These are encouraging results as the most prevalent effects of the wheel-terrain interface (i.e., traction) are wheel slip and sinkage. As shown in Section 2.5.4 this test was conducted to show the sinkage effects from a vehicle in constant slip.

Figure 4-7 shows that when the treated soils' compressive strength increases, as does its resistance to sinkage. This relationship is consistent with expectations as compressive strength and shear strength are the two main soil strength parameters influencing traction of a wheeled vehicle.

Additionally, figures 3-6, 3-7 and 3-8 in the previous chapter appear to show that as the rut created by the traction tester surpassed the crust depth, the rate of sinkage increased. This may indicate that much of the sinkage resistance comes from the hardened crust at the surface.

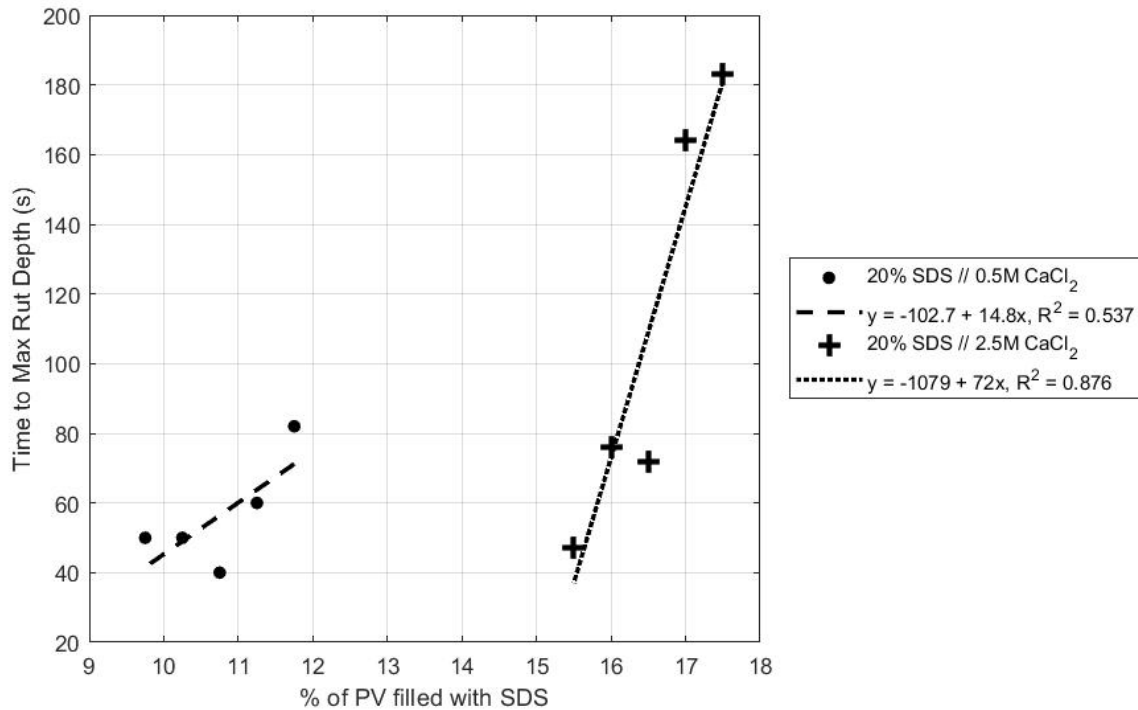


Figure 4-5. Plot of Time to Max Rut Depth results. Note: Regression only applies within the bounds of each dataset.

Table 4-2. Rate of sinkage (i.e., sinkage slope) from sandbox testing Round 1 (20% SDS // 2.5M CaCl₂)

% of PV filled with SDS	17.50%	17.00%	16.50%	16.00%	15.50%
Sinkage slope	0.016456	0.016006	0.052557	0.048445	0.079836
R squared	0.966	0.965	0.993	0.93	0.895
Compressive Strength (psi)	26.91	17.36	3.47	N/A	N/A

Note: Compressive strength values are 21 day averages from penetrometer testing.

Table 4-3. Rate of sinkage (i.e., sinkage slope) from sandbox testing Round 2 (20% SDS // 0.5M CaCl₂)

% of PV filled with SDS	11.75%	11.25%	10.75%	10.25%	9.75%
Sinkage slope	0.051414	0.071591	0.10028	0.077273	0.070909
R squared	0.968	0.955	0.978	0.966	0.966
Compressive Strength (psi)	59.03	52.09	25.70	13.89	17.36

Note: Compressive strength values are 21 day averages from penetrometer testing.

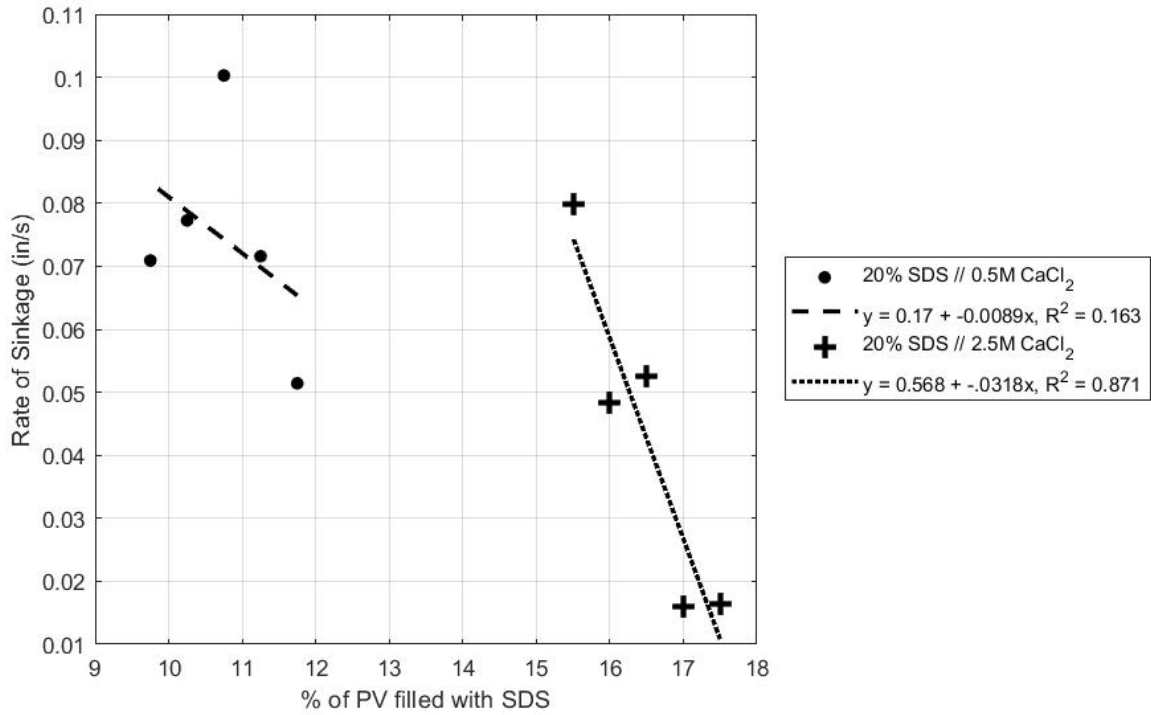


Figure 4-6. Rate of sinkage plotted as a function of SDS quantity. Note: Regression only applies within the bounds of each dataset.

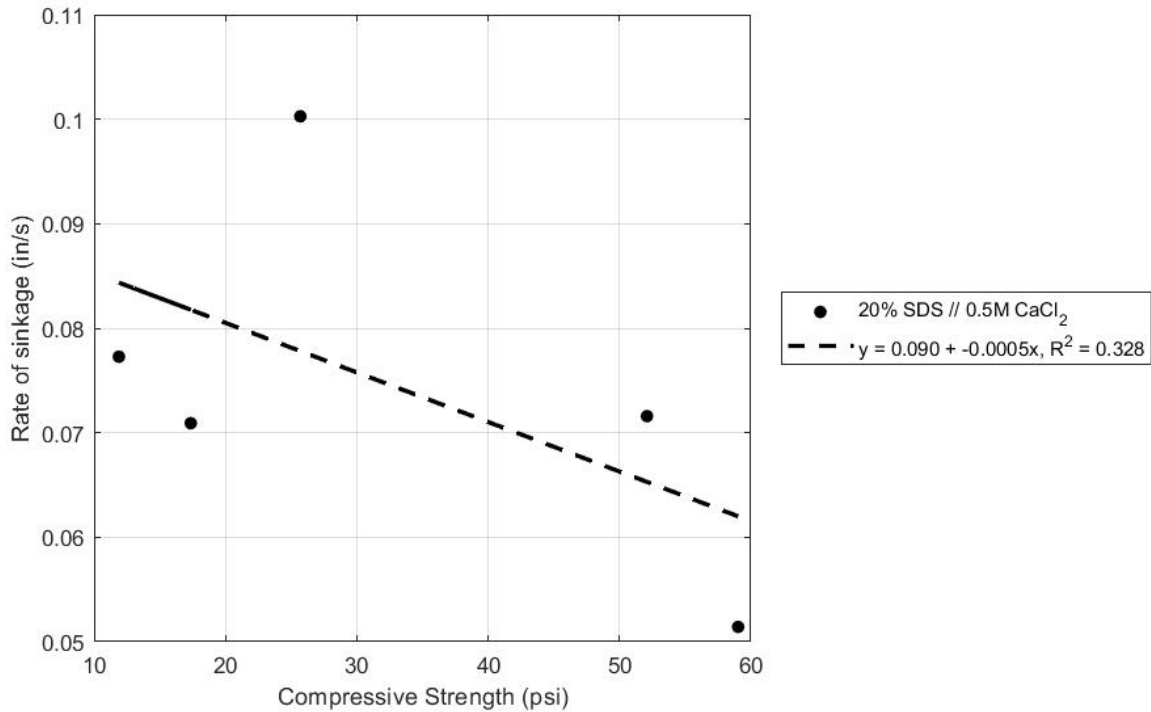


Figure 4-7. Rate of sinkage plotted as a function of Compressive Strength. Results from Round 2 of sandbox testing (20% SDS solution // 0.5M CaCl₂ solution). Note: Regression only applies within the bounds of the dataset.

4.3 Data Analysis – Crust Depth

Results from crust depth testing appeared to show that the thickness of stabilized sand at the surface tended to increase with increasing levels of SDS. This is shown in Figures 3-9 and 3-10. Additionally, the results from round 2 of sandbox testing (20% SDS // 0.5M CaCl₂) and control testing (no added CaCl₂) showed an apparent direct relationship between crust depth and compressive strength. This is shown in Figures 4-8 and 4-9 below. The results from round 1 of sandbox testing (20% SDS // 2.5M CaCl₂) were not plotted as only two treatment depth measurements were obtained.

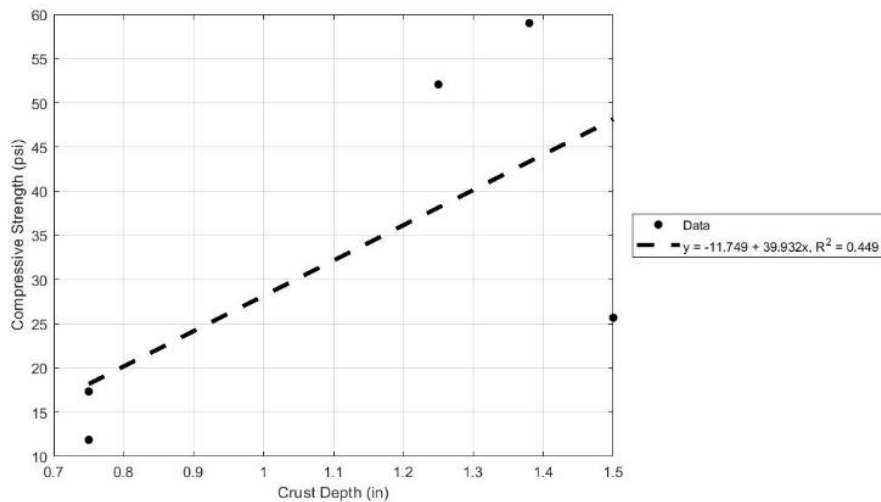


Figure 4-8. Plot of compressive strength vs crust depth for round 2 of sandbox testing (20% SDS solution // 0.5M CaCl₂ solution). Note: Regression only applies within the bounds of the dataset.

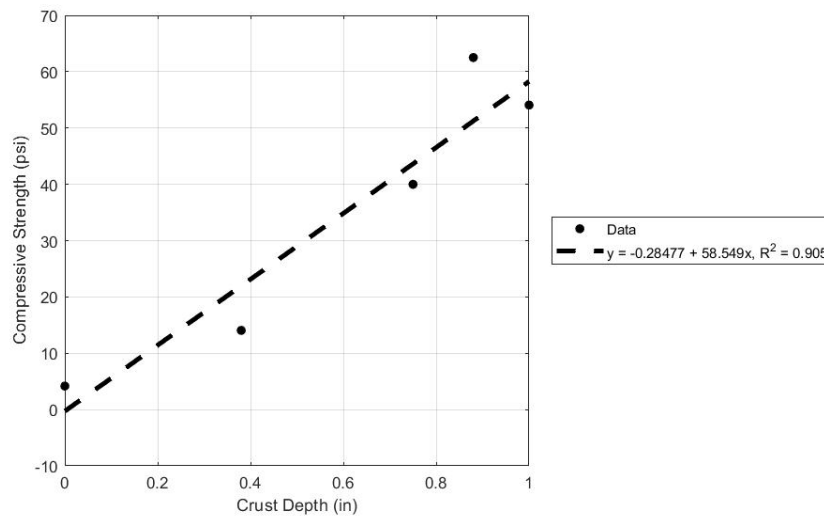


Figure 4-9. Plot of compressive strength vs crust depth for Control sandbox testing.
 Note: Regression only applies within the bounds of the dataset.

Unfortunately, these results are limited in the sense that researchers were not able to obtain depth measurements from multiple locations of the boxes. This was because the crust depth measurements were performed after the traction testing. The traction testing formed a rut hole that occupied much of the boxes' areas and broke much of the crust from the remaining areas. As such, crust measurements could only be performed far away from the rut holes – near the boxes' corners. It is possible that the crust under where the rut hole was formed may have had a different depth than the values measured far from the rut holes due to soil variability. Regardless, in general, a direct relationship was observed between SDS percentage and crust depth in the sense that more SDS appeared to form deeper crusts. However, it is important to note that in all cases, the crust depth was relatively small – in all cases less than 1.5 inches. It is unclear whether or not this limited effective treatment depth would be effective for naval landing vehicles in the field.

It is also important to note that when handling the stabilized crust, researchers noticed that those nearby tended to cough as a result of what appeared to be airborne SDS. This may be another indicator that SDS is reprecipitating in the soil, likely due to insufficient calcium.

4.4 Data Analysis – Dissolution Testing

The samples tested from the control boxes treated with SDS alone (D-8 through D-10) produced erratic results, one dissolving more quickly in seawater another more quickly in distilled water. Regardless, for each of the specimens treated with SDS alone, their stabilized structure completely broke down in less than 60 seconds. The variability in control testing may indicate that the SDS is bonding with varying levels of naturally occurring alkaline earth metals in the soil.

Results from dissolution testing varied based on the type of treatment. Test D-1 through D-3 (treated cylinders) and D-5 through D-7 (treated sand boxes) were treated with same constituent levels however much different results were observed. The cylinders used for D-1 through D-3 were somewhat friable prior to testing and dissolved rapidly in both seawater and distilled water. The fact that these cylinders were friable prior to testing is consistent with the cylinders that were prepared with similar treatment levels for UCS testing. The crust samples used for D-5 through D-7, however, were well stabilized prior to dissolution testing and held their structure really well in both seawater and distilled water. These results are shown in Figure 4-10. Researchers expected the samples to be insoluble in distilled water, but the data suggested the opposite – distilled water caused faster dissolution than seawater. Previously, Davies (2018) showed that specimens were relatively insoluble when immersed in freshwater. But, Davies' (2018) tests were conducted on cylinders with relatively high SDS quantities. It would appear

that decreasing SDS quantity and changing the treatment method to a surface percolation method increases dissolvability. In the context of USN field exercises, this is not necessarily a problem since the goal would be to return a beach to its native state after field exercises are conducted. But, in the context of more long-term stabilization, these points about solubility are important to note.

Overall, results shown here appear to indicate that CDS complexes are formed as a result of treating the sand with both SDS and CaCl₂, and the stabilized sand is subsequently resistive to dissolution in both seawater and distilled water.

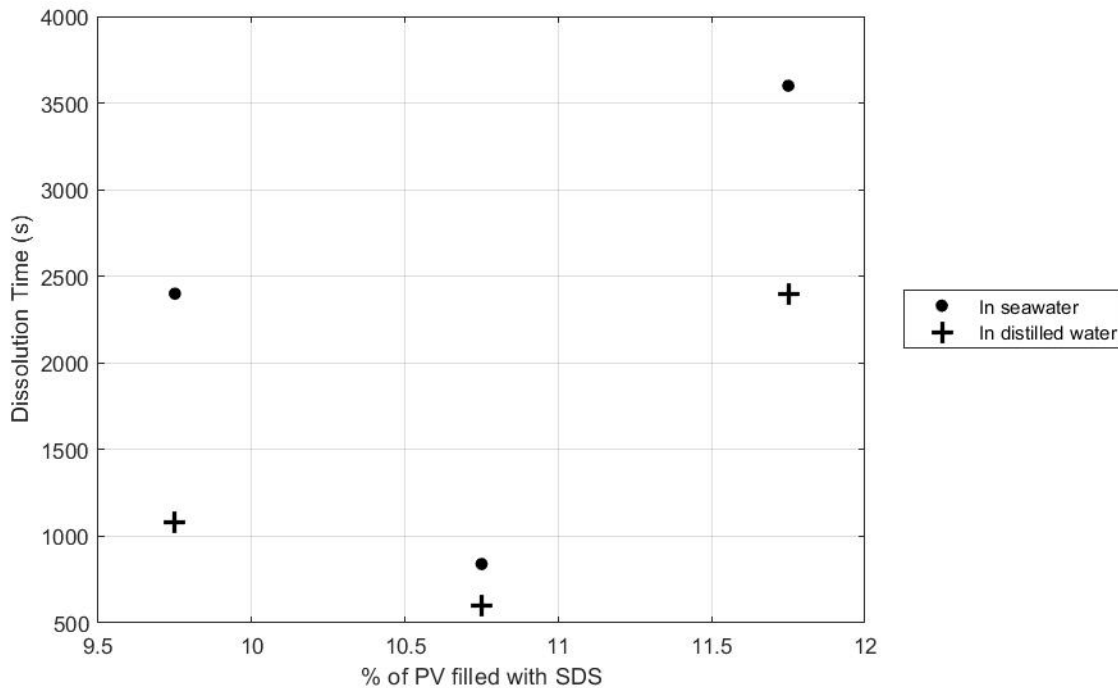


Figure 4-10. Plot of dissolution time vs SDS quantity

4.5 Implications for Upscaling to Field Application

- In this study, all treatment specifications were expressed as a function of the PV. In the field, the PV is infinite. Despite this, results here are useful in the sense

that when SDS solution as used in commercially available concentrations, in general, results showed “more is better.” As such, if this technology were to be upscaled, results here imply that adding as much SDS as possible to the soil matrix would produce the best results.

- It was found during testing that corrosion formed on steel surfaces that had been directly exposed to the treatment mixture. This could be problematic for the wheeled vehicles driving over SISS treated surfaces. This unexpected side effect is likely due to residual sodium and chlorine ions that were left over after the dodecyl sulfate-calcium-dodecyl sulfate reactions. Sodium and chloride in solution (i.e., saltwater) are known to increase electrical conductivity. It would appear that this increase in electrical conductivity increased the speed of the corrosion reaction where two electrons are removed from iron atoms and the result is precipitated iron oxide. Interestingly, the positively charged iron atoms did not appear to bond with the dodecyl sulfate tails – this point bears further investigation. To mitigate this potential issue in the future, it may be beneficial to use a different alkaline earth metal source in future tests.
- SDS powder is extremely fine and presents an inhalation hazard when it becomes airborne. This does not present an issue when it is dissolved in a solution. However, researchers noticed that once the treated sand had dried out and traction testing was conducted, the SDS precipitate tended to become airborne and induce minor coughing to those nearby. As stated earlier, this may be a result of insufficient calcium and may be mitigated by adding more CaCl_2 during treatment. Again, future work will be aimed at flooding additional

specimens with calcium in quantities that are much greater than the 2:1 stoichiometric ratio discussed in Chapter 2.

CHAPTER 5 CONCLUSIONS

5.1 Summary

This research was conducted to examine strength improvement and traction improvement in beach sand in the context of optimizing SISS constituent quantities (SDS and calcium). This was accomplished through two phases of testing. The first phase utilized testing cylinders and a UCS testing device to generate preliminary information about optimal quantities of SDS and calcium in beach sand. The second phase involved upscaling SISS treatment to bench-scales using sandboxes. This phase examined soils' compressive strength and tire rut formation with different quantities of SISS constituents when using treatment techniques that could be feasibly applied in the field. Research concluded with an examination of SISS-treated soil's dissolvability in both freshwater and saltwater.

5.3 Preliminary Conclusions

- Treating beach sand with SDS increased its compressive strength when using two different application methods – both mixing and percolation, and strength tended to increase with increasing amounts of SDS and longer dry times.
- At bench scales beach sand tended to become more resistive to wheeled vehicle sinkage as the amount of SDS added to the soil was increased. It is unclear whether or not this would be effective for full scale, naval vehicles in the field.
- Beach sand treated with both SDS and CaCl_2 was resistive to dissolution in both seawater and distilled water.
- It appears that some portion of the strength and traction improvements seen in this research is due to dodecyl sulfate-calcium-dodecyl sulfate reactions and

another portion is due to reprecipitated SDS. This reprecipitated SDS could be a result of insufficient calcium and may be mitigated by adding more CaCl_2 during treatment. This point bears further investigation.

5.3 Recommendations for Future Testing

This study served as a preliminary assessment of the SISS treatment technique. As such significant future research is required. Additional testing recommendations are as follows:

- Flood specimens with calcium in quantities that are much greater than the 2:1 stoichiometric ratio. This may help activate additional calcium and drive more SISS chemical reaction.
- Test the effects of using different alkaline earth metals (e.g. magnesium and strontium) beyond the preliminary testing reported in Davies (2018)
- Treat “clean” Ottawa sand and conduct scanning electron microscopy (SEM) and x-ray diffraction (XRD) analyses to better determine the mechanisms associated with the observed strength improvements.
- Test various dry times and other environmental inputs such as exposure to direct sunlight, rain, and variations in temperature.
- Test shear strength using a triaxial shear test, direct shear test or bevameter. These tests may provide additional bench-scale results prior to full scale testing.
- Test the thrust exerted on the soil from the testing vehicle. This could be done using a similar setup as that used for the traction testing in this study, only place the sandbox on rollers and a scale on back horizontal surface of the box.

LIST OF REFERENCES

- ASTM (2014). Standard Test Method for Rapid Determination of Carbonate Content of Soils. ASTM International West Conshohocken, PA.
- ASTM (2014). Standard Test Methods for Specific Gravity of Soil Solids by Water Pycnometer. ASTM International West Conshohocken, PA.
- ASTM (2014). Standard Test Method for Sieve Analysis of Fine and Coarse Aggregates. ASTM International West Conshohocken, PA.
- ASTM (2016). Standard Test Method for Unconfined Compressive Strength of Cohesive Soil. ASTM International West Conshohocken, PA.
- Chek, A., Crowley, R.W., Ellis, T.N., and Durnin, M. (2020). An evaluation of factors affecting erodibility improvement for MICP-treated beach sand. *Journal of Geotechnical and Geoenvironmental Engineering*, DOI: 10.1061/(ASCE)GT.1943-5606.0002481.
- Center for Seabees and Facilities Engineering (CSFE). (2010). Soil Stabilization. In *ENGINEERING AID ADVANCED NAVEDTRA 14336A* (p. 13-6). Retrieved from http://navybmr.com/study%20material/14336a/14336A_ch13.pdf
- Crowley, R. (2018, August). An Assessment of Hydraulic Damages in Northeast Florida from Hurricane Irma. Presentation presented at the National Hydraulic Engineering Conference, Columbus, OH, USA. Retrieved from <https://www.youtube.com/watch?v=-DA2De-9qno>
- Crowley, R., Hudyma, N., Sharma, R., Akan, C., Brown, C., Dally, W., Song, X. (2017). Geotechnical damage in central and northeastern Florida from Hurricane Irma. 10.18118/G6DQ0J.
- Crowley, R., Davies, M.*, and Hudyma, N. (2019). Method of strengthening soil via chemical inducement. US Patent 62/873,042, filed July 11, 2019.
- Cummings, David and Kenton, Frank J. (2004) Eleven Case Studies of Failures in Geotechnical Engineering, Engineering Geology, and Geophysics: How They Could Have Been Avoided. International Conference on Case Histories in Geotechnical Engineering. 1. <https://scholarsmine.mst.edu/icchge/5icchge/session07/1>
- Davies, M. (2018). Soil Improvement Using Microbial Induced Calcite Precipitation and Surfactant Induced Soil Strengthening. *UNF Graduate Theses and Dissertations*. 837. <https://digitalcommons.unf.edu/etd/837>
- Davies, M., Crowley, R., Ellis, T. N., Hudyma, N., Ammons, P., and Matemu, C. Wasman, S., Yahaya, M., Ford, J., Zimmerman, A. (2019). Microbially Induced Calcite Precipitation Using Surfactants for the Improvement of Organic Soil." Proc., Geo-Congress 2019.

Ebid, Ahmed. (2018). Mathematical Approach to Simulate Soil Behavior Under Shallow Compaction. *International Journal of Scientific and Engineering Research*. 9.

Evans, I. (1964). The sinkage of tracked vehicles on soft ground. *Journal of Terramechanics*, 1(2), 33–43. [https://doi.org/10.1016/0022-4898\(64\)90063-1](https://doi.org/10.1016/0022-4898(64)90063-1)

Geoengineer.org. (2020, June 15). *Stunning footage of foundation failure that causes 3-story building to collapse in India*. <https://www.geoengineer.org/news/stunning-footage-of-foundation-failure-that-causes-3-story-building-to-collapse-in-india>

Habiba Afrin. (2017). A Review on Different Types Soil Stabilization Techniques. *International Journal of Transportation Engineering and Technology*. Vol. 3, No. 2, 2017, pp. 19-24. doi: 10.11648/j.ijtet.20170302.12

Hollis, J. (2014, September 8). Cherry Point Marines repair MCAF taxiway with new AM-2 matting. Retrieved September 21, 2020, from <https://www.quantico.marines.mil/News/News-Article-Display/Article/518481/cherry-point-marines-repair-mcaf-taxiway-with-new-am-2-matting/>

Landon, M. E., Hudyma, N. W., Sharma, R. S. (2020). Hurricane Irma: Consequences of Intense Rainfall and Storm Surge from a Tropical Storm in North and Central Florida, Vol. 5, Issue 4, p.26-46. doi: 10.4417/IJGCH-05-04-02

Lyasko, M. (2010). Slip sinkage effect in soil–vehicle mechanics. *Journal of Terramechanics*, 47(1), 21–31. <https://doi.org/10.1016/j.jterra.2009.08.005>

Martin, D., Dodds, K., Ngwenya, B. T., Butler, I. B., & Elphick, S. C. (2012). Inhibition of *Sporosarcina pasteurii* under Anoxic Conditions: Implications for Subsurface Carbonate Precipitation and Remediation via Ureolysis. *Environmental Science & Technology*, 46(15), 8351–8355. <https://doi.org/10.1021/es3015875>

Mullins, G., & Gunaratne, M. (2015, October). *Soil Mixing Design Methods and Construction Techniques for Use in High Organic Soils* (Final Report). Tampa, FL: University of South Florida.

Reina, G., Ojeda, L., Milella, A., & Borenstein, J. (2006). Wheel slippage and sinkage detection for planetary rovers. *IEEE/ASME Transactions on Mechatronics*, 11(2), 185–195. <https://doi.org/10.1109/tmech.2006.871095>

Rushing, T. W., Garcia, L., Tingle, J. S., Allison, P. G., & Rutland, C. A. (2014, September). *AM2 3-4 Alternate Lay Pattern Evaluation*. US Army Corps of Engineers, Engineer Research and Development Center. Retrieved from <https://apps.dtic.mil/dtic/tr/fulltext/u2/a610771.pdf>

Schmitz, K. S. (2018). *Physical Chemistry*. <https://doi.org/10.1016/B978-0-12-800513-2.00004-8>

Schreiber, M., & Kutzbach, H. D. (2008). Influence of soil and tire parameters on traction. *Research in Agricultural Engineering*, 54(No. 2), 43–49.
<https://doi.org/10.17221/3105-rae>

Sputnik. (2015, October 22). *While Russian Warplanes Bomb Terrorists, NATO Gets Stuck on a Sandy Beach*. Sputnik International.
<https://sputniknews.com/europe/201510211028896927-nato-portugal-beach-stuck/>

Wikar, K. C., & Hill, J. R. (Eds.). (2018). *Wick Drains for Soil Consolidation and Environmental Remediation at The Atlantic Wood Superfund Site, Portsmouth, Va.* Retrieved from
https://www.westerndredging.org/phocadownload/2018_Norfolk/Proceedings/5b-2.pdf

BIOGRAPHICAL SKETCH

Josh Sasser is a native of Pace, Florida. He graduated from the University of Central Florida in May 2011 earning a Bachelor of Science in Civil Engineering. He was then commissioned into the United States Navy through Officer Candidate School in Newport, Rhode Island in October 2011.

His assignments in Navy include: Company Commander and Detachment Officer-in-charge for Naval Mobile Construction Battalion ONE; Task Force Engineer for Combined Joint Special Operations Task Force Iraq; Combat Engineer for SEAL Team EIGHT; and Construction Manager for the Naval Research Laboratory, Joint Base Andrews, and Naval Station Mayport.

Josh is a registered professional engineer in the state of Arizona. In 2018 he was selected into the Navy's Ocean Facilities Program and is currently a graduate student at the University of North Florida where he is pursuing a master's degree in Coastal and Port Engineering. Josh and his wonderful wife, Kati, have two amazing children, Clay and Savannah.